RESEARCH ARTICLE SUMMARY

IMMUNOLOGY

Recurrent infection progressively disables host protection against intestinal inflammation

Won Ho Yang, Douglas M. Heithoff, Peter V. Aziz, Markus Sperandio, Victor Nizet, Michael J. Mahan, Jamey D. Marth*

INTRODUCTION: Foodborne infections represent a serious and increasing human health problem while at the same time the incidence and prevalence of colitis and the inflammatory bowel diseases (IBDs) are increasing. The origins of these life-threatening syndromes predominantly include environmental factors deduced from studies of genetic twins and other human populations. Pathogen infection has been postulated as a possible environmental trigger of chronic intestinal inflammation and colitis. The *Salmonella* bacterial pathogen, for example, is widespread throughout the environment and remains a leading cause of human foodborne illness and disease. *Salmonella* infection can occur by the ingestion of contaminated food products often resulting in acute but temporary intestinal discomfort and dysfunction.

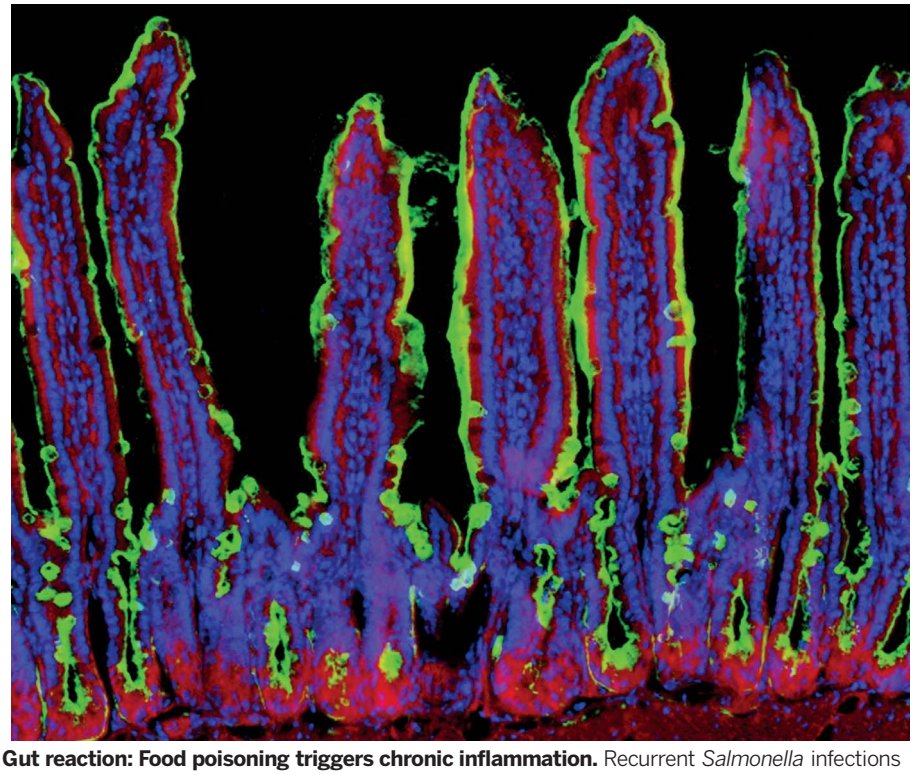
RATIONALE: Possible links between pathogen infections and chronic intestinal inflammation are under increased study. Bacterial infections have been associated with seasonal increases in hospital admissions diagnosing intestinal inflammation and the IBDs. We considered that common repeated infections such as may occur in human food poisoning by *Salmonella* might be involved in triggering chronic intestinal inflammation. Such infections could be relatively mild, causing few symptoms that go unreported and disappear without clinical intervention, making it possible that there is currently an underappreciation of the numbers of infections occurring among individuals over a life span. We investigated whether low-titer and nonlethal *Salmonella* infections, designed to model repeated episodes of human food poisoning, may lead to chronic intestinal inflammation and colitis. If so, such a mechanism might be responsible for triggering human inflammatory syndromes including colitis and IBDs.

RESULTS: We developed and characterized a model of human food poisoning in the mouse using recurrent low-dose and nonlethal gastrointestinal infections of a virulent *Salmonella* isolate. We observed that repeated exposure induced inflammation of intestinal tissues, especially the colon. Although the host effectively cleared the pathogen weeks before reinfection, inflammation and intestinal tissue damage progressively increased in severity with additional infections. In addition, after the cessation of additional infections, inflammation and tissue damage failed to subside and persisted for months throughout the duration of study. We have identified the disease mechanism to be an acquired deficiency of intestinal alkaline phosphatase (IAP), an enzyme produced by enterocytes of the duodenum of the small intestine. IAP dephosphorylates and detoxifies the lipopolysaccharide (LPS) endotoxin produced by commensal microbiota of the host. *Salmonella* infection induced endogenous neuraminidase (Neu) activity among enterocytes of the duodenum by a Toll-like receptor 4 (TLR4)–dependent mechanism. This elevation of Neu activity accelerated the molecular aging and turnover of IAP, causing IAP deficiency in the colon. IAP deficiency led to elevated levels of LPS-phosphate that provoked TLR4-dependent inflammation. IAP augmentation or neuraminidase inhibition using a marketed antiviral neuraminidase inhibitor were similarly effective at preventing the accumulation of LPS-phosphate and the onset of disease.

CONCLUSION: We have discovered an environmental and pathogenic origin of chronic intestinal inflammation using a model of recurrent human food poisoning. We further show that this disease can be prevented by either IAP augmentation or Neu inhibition, both of which may represent prophylactic and therapeutic approaches to human colitis and the IBDs. ■

ON OUR WEBSITE

Read the full article at http://dx.doi.org/10.1126/science.aao5610



Gut reaction: Food poisoning triggers chronic inflammation. Recurrent *Salmonella* infections progressively induce host Neuraminidase 3 (green) on the surface of enterocytes among duodenal epithelial cells of the small intestine. Epithelial cells are counterstained to also visualize DNA among cell nuclei (blue) and the cytoskeleton component α-tubulin (red). Elevated neuraminidase activity accelerates the molecular aging and clearance of IAP in triggering colitis.

The list of author affiliations is available in the full article online.
*Corresponding author. Email: jmarth@sbpdiscovery.com
Cite this article as W. H. Yang *et al.*, *Science* **358**, eaao5610 (2017). DOI: 10.1126/science.aao5610

Downloaded from http://science.sciencemag.org/ on December 21, 2017

RESEARCH ARTICLE

IMMUNOLOGY

Recurrent infection progressively disables host protection against intestinal inflammation

Won Ho Yang,[1,2,3] Douglas M. Heithoff,[1,3] Peter V. Aziz,[1,2,3] Markus Sperandio,[4] Victor Nizet,[5] Michael J. Mahan,[1,3] Jamey D. Marth[1,2,3]*

Intestinal inflammation is the central pathological feature of colitis and the inflammatory bowel diseases. These syndromes arise from unidentified environmental factors. We found that recurrent nonlethal gastric infections of Gram-negative *Salmonella enterica* Typhimurium (ST), a major source of human food poisoning, caused inflammation of murine intestinal tissue, predominantly the colon, which persisted after pathogen clearance and irreversibly escalated in severity with repeated infections. ST progressively disabled a host mechanism of protection by inducing endogenous neuraminidase activity, which accelerated the molecular aging and clearance of intestinal alkaline phosphatase (IAP). Disease was linked to a Toll-like receptor 4 (TLR4)–dependent mechanism of IAP desialylation with accumulation of the IAP substrate and TLR4 ligand, lipopolysaccharide-phosphate. The administration of IAP or the antiviral neuraminidase inhibitor zanamivir was therapeutic by maintaining IAP abundance and function.

Inflammation of the intestinal tract is the defining feature of colitis and the human inflammatory bowel diseases (IBDs), including Crohn's disease and ulcerative colitis (UC). In these syndromes, chronic inflammation disrupts intestinal homeostasis and provokes immune-mediated tissue damage (*1*–*3*). The origins of these diseases remain mysterious and involve one or more environmental factors (*4*). Among multiple human monozygotic twin comparisons, the genetic contribution to the origin of UC is about 20%, whereas in Crohn's disease, genetics may play a larger though often minor role (*5*). Considering the possible environmental origins of disease, pathogenic infection has been studied as a factor in precipitating intestinal inflammation (*6*). Notably, bacterial infections have been linked to seasonal increases in hospital admissions involving intestinal inflammation and IBD (*7*).

Small-inoculum bacterial infections that are brief and self-limited are likely to be the most common infections, and they may frequently go unreported, potentially leading to an underappreciation of the numbers of infections among individuals. We hypothesized that there may be cumulative effects of repeated small-inoculum and subclinical infections, which, if true, may be detected in a model of human food poisoning. We designed a study using recurrent low-titer nonlethal gastrointestinal infection by the bacterium *Salmonella enterica* Typhimurium (ST), a common human pathogen. Nontyphoidal *Salmonella* (NTS) produces a greater human disease burden than any other foodborne bacterial pathogen in the United States, causing more than a million illnesses annually (*8*, *9*). Globally, NTS causes 93.8 million cases and 155,000 deaths each year (*10*) and is responsible for up to 50% of bacteremias in young children from developing countries (*11*, *12*).

Results

ST infection elicits intestinal inflammation by diminishing host intestinal alkaline phosphatase levels

Beginning at 8 weeks of age, wild-type C57BL/6J mice were infected by gastric intubation with 2×10^3 ST colony-forming units (CFU) every 4 weeks for six consecutive months. After infection, ST was detected transiently and predominantly in the small intestine and some lymphoid tissues. The pathogen was cleared by the host to undetectable levels by 21-days post-infection monitoring, which further noted the absence of overt symptoms or mortality among the animals (fig. S1, A and B). The onset of disease required more than a single infection with this low titer, whereas multiple signs of disease were evident among most of the animals before the fourth infection. Phenotypes consistent with the onset of intestinal dysfunction included weight loss, reduced colon length, altered stool consistency (diarrhea), and the presence of fecal blood (Fig. 1, A to D, and fig. S1C). By 20 weeks of age and before the fourth infection, signs of disease were present among most of the animals and further included an epithelial barrier defect (Fig. 1E). At 32 to 48 weeks, rectal prolapse was observed among some animals undergoing recurrent infections (Fig. 1F). The frequency of disease symptoms escalated with successive recurrent infections and persisted for at least 5 months after the cessation of infections.

Reductions in alkaline phosphatase (AP) activity and intestinal AP (IAP) abundance were detected in both the small intestine and intestinal contents, whereas levels of duodenal tissue mRNA encoding IAP were unchanged (Fig. 1, G to I, and fig. S2A). Mammalian IAP is produced exclusively by enterocytes of the duodenum and is released from the cell surface into the lumen where it can dephosphorylate and thereby detoxify the lipopolysaccharide (LPS) endotoxin of Gram-negative bacteria (*13*–*16*). We found that oral supplementation with calf IAP (cIAP) maintained normal AP activity levels in the intestinal tract among animals receiving recurrent ST infections (Fig. 1J). Analysis of LPS isolated from the intestinal tract at 20 weeks of age before the fourth infection and after ST clearance revealed a fourfold increase in endogenous LPS-phosphate levels in the context of a 50% increase in total LPS, both of which were maintained close to normal levels in mice receiving cIAP treatment (Fig. 1K). Augmentation of AP activity by cIAP treatment also protected against the development of disease symptoms encompassing weight loss, colon length, diarrhea, fecal blood, and epithelial barrier function (Fig. 1L).

Inflammatory cytokines associated with intestinal tissue inflammation include chemokine ligand 5 (CCL5), interleukin-1β (IL-1β), tumor necrosis factor–α (TNF-α), and interferon-γ (IFN-γ). Recurrent ST infection progressively increased inflammatory cytokine mRNA expression levels predominantly in the colon, unless cIAP treatment was provided (Fig. 1M). Histopathological changes were also predominantly seen in the colon, including an infiltration of leukocytes into the lamina propria, which included neutrophils, monocytes, and T cells, as well as an erosion of the epithelial barrier, and reduced goblet cell numbers, whereas a much lesser effect was observed in the small intestine and, in addition, only in the ileum (Fig. 1N and figs. S2B and S3). Thus, recurrent nonlethal gastrointestinal infection of ST diminished the expression of host IAP activity that normally confers host protection against intestinal inflammation and tissue damage predominantly in the colon. Studies were further undertaken to identify the mechanisms that regulate IAP function.

IAP deficiency is linked to an accelerated rate of desialylation and endocytic localization

IAP is synthesized as a glycosylphosphatidylinositol (GPI)–linked glycoprotein residing on the

[1]Center for Nanomedicine, University of California, Santa Barbara, Santa Barbara, CA 93106, USA. [2]Sanford Burnham Prebys Medical Discovery Institute, University of California, Santa Barbara, Santa Barbara, CA 93106, USA. [3]Department of Molecular, Cellular, and Developmental Biology, University of California, Santa Barbara, Santa Barbara, CA 93106, USA. [4]Walter-Brendel-Centre for Experimental Medicine, Ludwig-Maximilians-University, Munich, Germany. [5]Department of Pediatrics and Skaggs School of Pharmacy and Pharmaceutical Sciences, University of California, San Diego, La Jolla, CA 92093, USA.
*Corresponding author. Email: jmarth@sbpdiscovery.com

Downloaded from http://science.sciencemag.org/ on December 21, 2017

enterocyte cell surface of the duodenum until it is released into the intestinal lumen by phospholipase activity (*13*, *17*). IAP production was investigated by pulse-chase experiments of ex vivo primary enterocyte cultures derived from small intestinal tissue. Normal rates of IAP synthesis and appearance at the cell surface were observed among all enterocyte cultures regardless of previously cleared infections (Fig. 2A). In contrast, a significant decrease in IAP cell surface half-life with reduced IAP abundance in the culture media was measured among enterocyte samples from mice that had cleared multiple infections (Fig. 2, B and C). Colocalization studies revealed increased colocalization of IAP with markers of early endosomes and lysosomes coincident with reduced cell surface IAP abundance (Fig. 2, D and E).

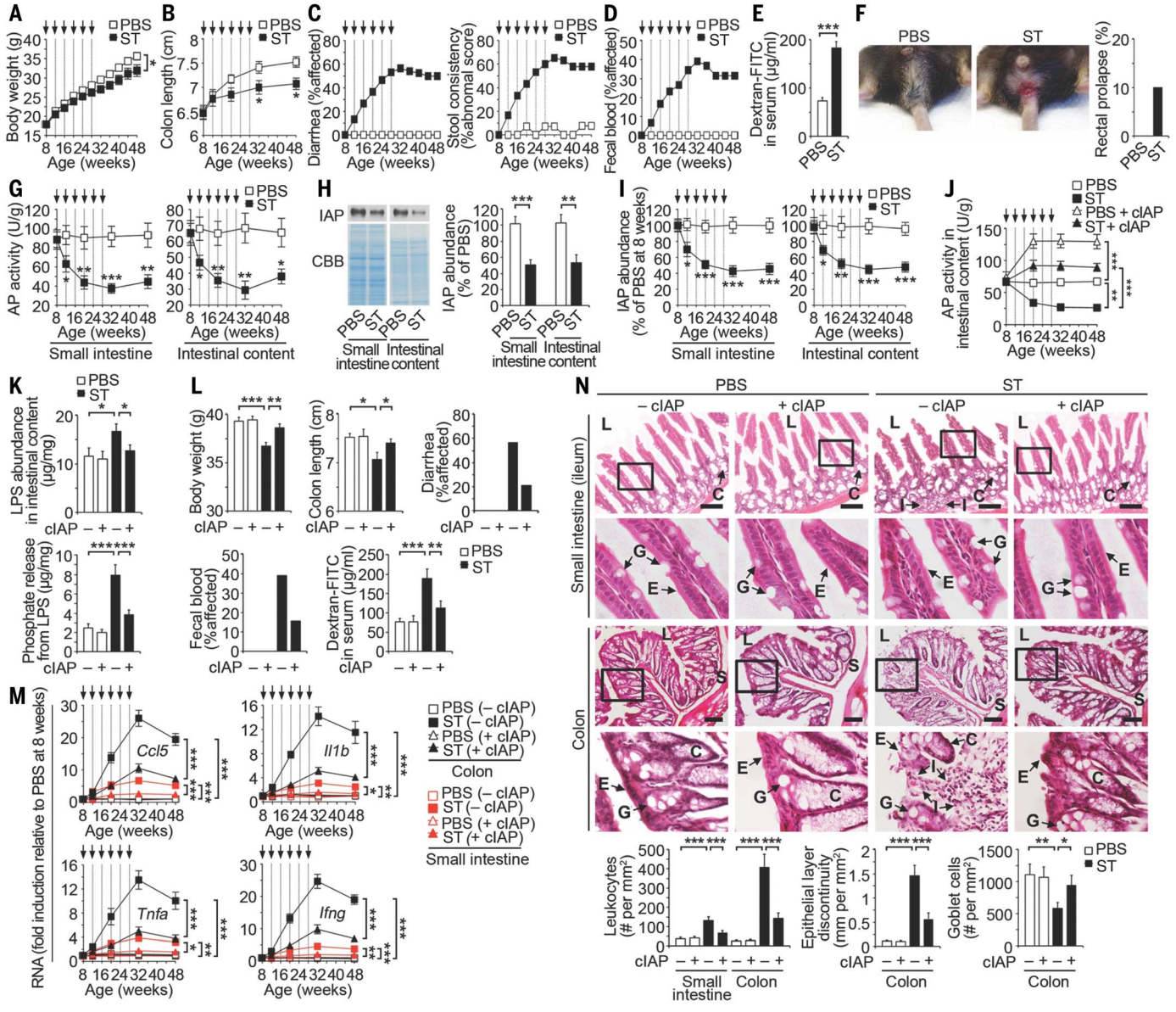


Fig. 1. Recurrent ST infection diminishes the abundance and protective role of IAP. Wild-type (WT) mice were analyzed during a course of recurrent ST infection (2×10^3 CFU) or uninfected [phosphate-buffered saline (PBS)] at indicated time points (arrows). (**A**) Body weight (ST, $n = 20$; PBS, $n = 19$). (**B**) Colon length ($n = 40$ per condition). (**C**) Diarrhea and stool consistency (ST, $n = 19$; PBS, $n = 13$). (**D**) Fecal blood (ST, $n = 19$; PBS, $n = 13$). (**E**) Intestinal epithelial barrier function ($n = 8$ per condition) at 20 weeks of age before the fourth infection. FITC, fluorescein isothiocyanate. (**F**) Rectal prolapse (ST, $n = 30$; PBS, $n = 20$) at 32 to 48 weeks of age or 4 to 20 weeks after last ST infection (representative image). (**G**) AP activity ($n = 40$ per condition). (**H**) Immunoblot blot analysis of IAP at 20 weeks of age before the fourth infection ($n = 8$ per condition). (**I**) Relative IAP abundance ($n = 40$ per condition). (**J**) AP activity ± cIAP ($n = 40$ per condition). (**K**) LPS abundance and phosphate released from LPS ($n = 8$ per condition) at 20 weeks of age. (**L**) Body weight ($n = 10$ per condition), colon length ($n = 8$ per condition), diarrhea (ST, $n = 23$; PBS, $n = 14$; ST + cIAP, $n = 19$; PBS + cIAP, $n = 15$), fecal blood (ST, $n = 23$; PBS, $n = 14$; ST + cIAP, $n = 19$; PBS + cIAP, $n = 15$) at 48 weeks of age (20 weeks after last ST infection), and intestinal epithelial barrier function ($n = 8$ per condition) at 20 weeks of age before the fourth infection. (**M**) Cytokine mRNA expression ($n = 30$ per condition). (**N**) Hematoxylin and eosin (H&E)–stained intestinal tissues at 48 weeks of age (20 weeks after last ST infection). L, intestinal lumen; E, epithelial layer; C, crypt; G, goblet cell; S, submucosa; I, infiltration of leukocytes. Graphs are representative of 16 fields of view ($n = 4$ per condition). All scale bars, 100 μm. Error bars represent means ± SEM. ***$P < 0.001$, **$P < 0.01$, and *$P < 0.05$; Student's t test (A, B, E, and G to I) or one-way analysis of variance (ANOVA) with Tukey's multiple comparisons test (J to N).

Downloaded from http://science.sciencemag.org/ on December 21, 2017

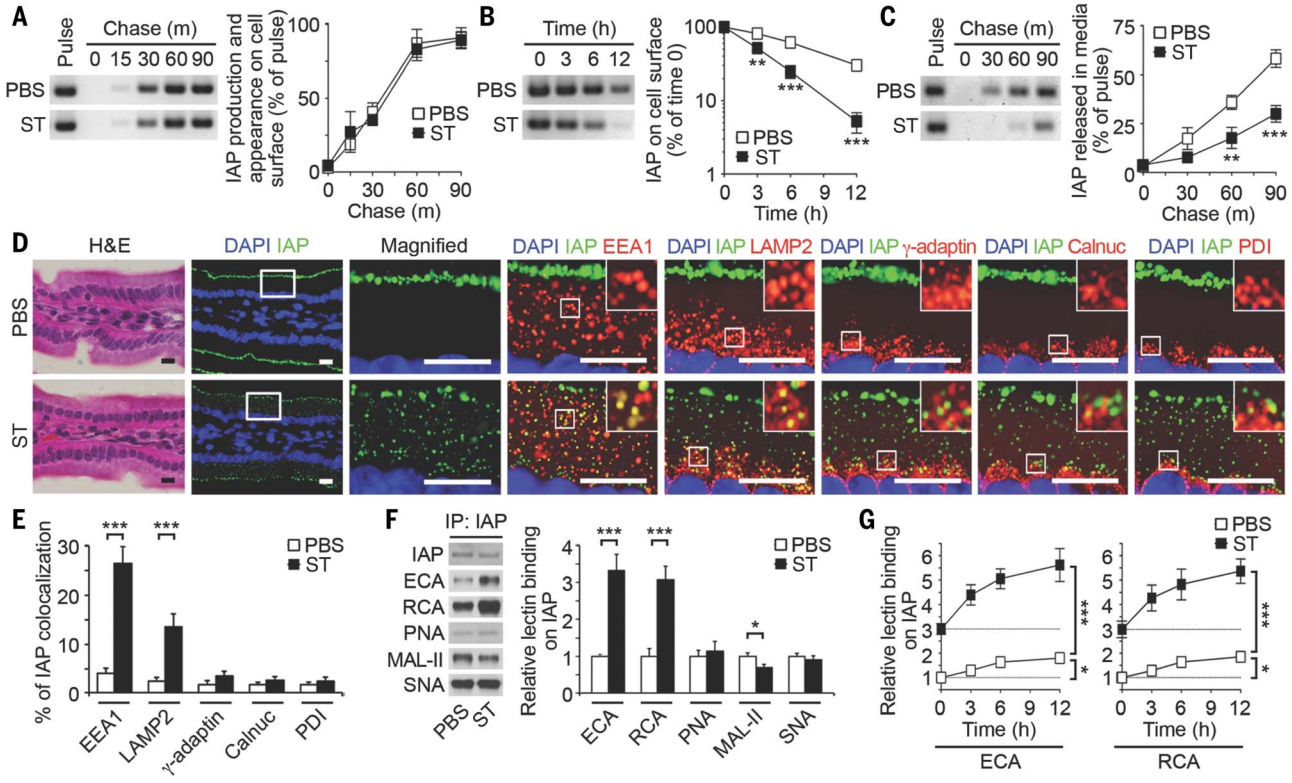


Fig. 2. Mechanism of IAP regulation during recurrent ST infection. (**A** to **C**) Pulse-chase analyses of IAP synthesis, trafficking, and cell surface half-life among cultured primary enterocytes isolated from WT mice at 20 weeks of age (before a fourth ST infection). (**D** and **E**) In situ localization and intracellular colocalization of IAP in duodenal sections stained with H&E or with fluorescent antibodies to IAP (green) and intracellular compartment proteins (red), including early endosomes (EEA1), lysosomes (LAMP2), trans-Golgi (γ-adaptin), cis-Golgi (Calnuc), or the endoplasmic reticulum (PDI), depicting the percentage of IAP colocalization (yellow). Graphs are representative of 10 fields of view (n = 4 per condition). Scale bars, 10 μm. DAPI, 4′,6-diamidino-2-phenylindole. (**F**) Lectin blot of IAP from small intestine. (**G**) Lectin binding of IAP on cultured enterocytes after cell surface biotinylation. (A to G) WT mice at 20 weeks of age before fourth infection. (A to C and G) n = 6 per condition. (F) n = 8 per condition. Error bars represent means ± SEM. ***P < 0.001, **P < 0.01, and *P < 0.05; Student's t test (A to C and E and F) or one-way ANOVA with Tukey's multiple comparisons test (G).

IAP is glycosylated during its synthesis in the secretory pathway. We next analyzed the glycan linkages attached to enterocyte IAP using analytical lectins, including the α2-3 sialic acid–specific lectin *Maackia amurensis* lectin II and the galactose-specific lectins *Erythrina cristagalli* agglutinin and *Ricinus communis* agglutinin. These lectins have been validated biochemically and genetically, although their binding does not provide full structural resolution of all glycan types and linkages present. A significant reduction of terminal sialic acid linkages coincident with the exposure of underlying galactose linkages was measured in the context of recurrent infection (Fig. 2F). No comparative changes to other specific glycan linkages were detected, including the sialylation state of core 1 O-glycans, or changes in abundance of α2-6–linked sialic acids, using peanut agglutinin and *Sambucus nigra* lectins, respectively. In the absence of infection, we observed a progressive desialylation of the glycans attached to nascent IAP on the enterocyte cell surface, indicative of a feature of its normal molecular aging. This basal rate of IAP desialylation was significantly increased by recurrent ST infection and was concurrent with increased IAP internalization and degradation in enterocytes (Fig. 2G). Although IAP deficiency appeared to be the predominant factor in disease onset, as indicated by the effects of cIAP treatment, multiple enterocyte cell surface glycoproteins were observed to be desialylated and internalized from the cell surface of endocytes, including sucrase-isomaltase, dipeptidyl peptidase 4, and lactase (fig. S4). These results suggest that the presence of one or more sialyltransferases establishes the normal half-lives (and consequent abundance) of enterocyte cell surface glycoproteins, including IAP.

ST3Gal6 is responsible for IAP sialylation in protecting against intestinal inflammation

The ST3Gal6 sialyltransferase generates α2-3 sialic acid linkages on glycoproteins and is highly expressed in the intestinal tract (*18*, *19*). In mice lacking a functional *St3gal6* gene, we detected a significant reduction in AP activity and IAP abundance, whereas mRNA encoding IAP was unchanged (Fig. 3, A and B, and fig. S5A). Although LPS levels in the intestinal tract were similar at 8 weeks of age, a threefold increase of LPS-phosphate abundance was measured, consistent with reduced AP activity (Fig. 3C). Because of absent ST3Gal6 function, IAP sialic acid linkages were also deficient with increased galactose exposure (Fig. 3D), similar to findings in wild-type mice experiencing recurrent ST infection. Glycan alterations were further detected histologically among small intestinal epithelial cells (fig. S5B). Diminished IAP sialylation in ST3Gal6 deficiency was linked to reduced IAP cell surface residency and increased IAP colocalization with markers of endosomes and lysosomes (Fig. 3, E to I). Thus, IAP sialylation by ST3Gal6 functions to maintain IAP half-life and abundance in the intestinal lumen. The impact of IAP deficiency caused by the absence of ST3Gal6 was further investigated.

Mice aging in the absence of ST3Gal6 was compared with that of wild-type littermates in the presence and absence of recurrent ST infection and cIAP therapy. Spontaneous phenotypes detected in uninfected mice lacking ST3Gal6 included reduced body weight, reduced colon length, diarrhea, the presence of fecal blood, and epithelial barrier dysfunction, all of which were exacerbated by recurrent ST infection. The addition of cIAP to drinking water normalized AP activity levels during adult life and reduced or eliminated signs of disease (Fig. 4, A to C). Similarly, increased LPS-phosphate levels were closely associated with

Downloaded from http://science.sciencemag.org/ on December 21, 2017

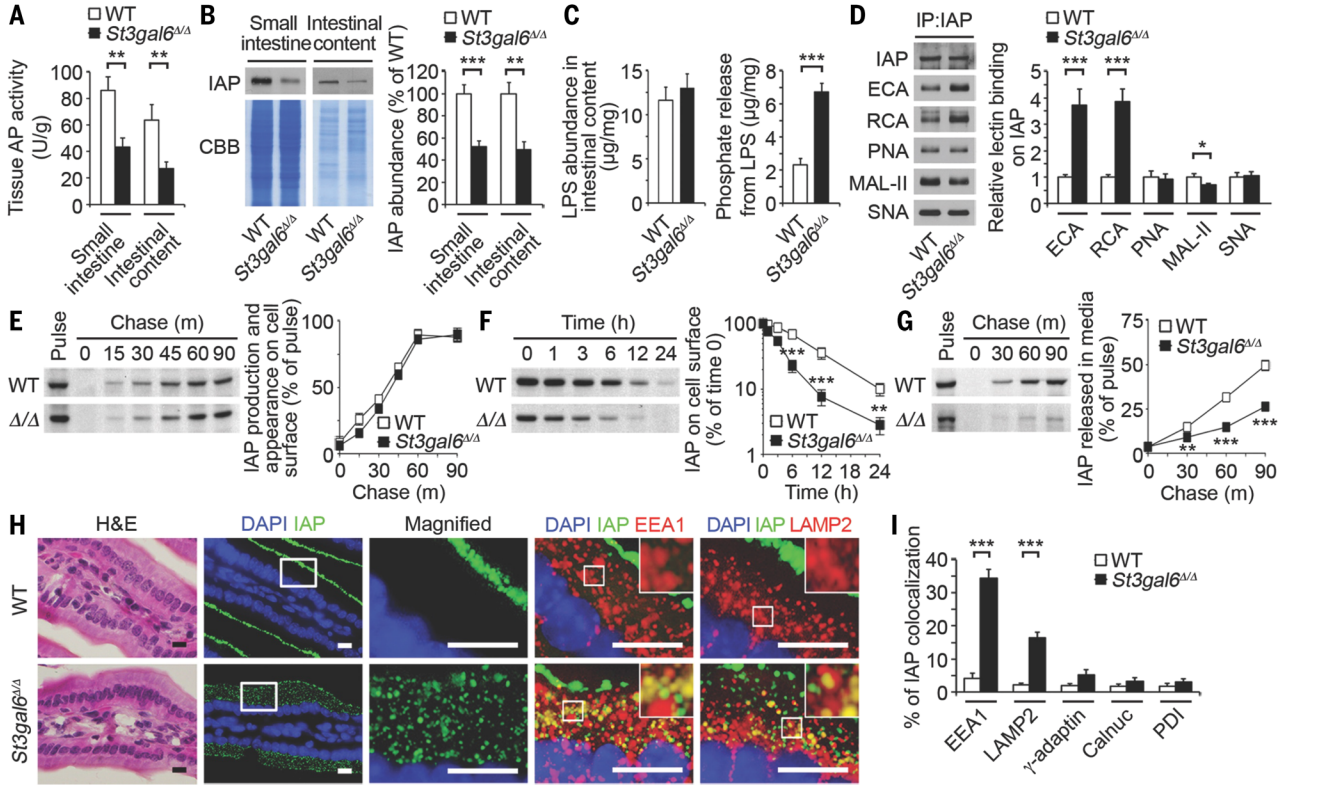


Fig. 3. Mechanism of IAP regulation by ST3Gal6 sialylation. (**A**) AP activity. (**B**) IAP protein abundance. (**C**) LPS abundance and phosphate released from LPS of intestinal content. (**D**) Lectin blot of IAP from small intestine. (**E** to **G**) Pulse-chase of IAP synthesis and trafficking and IAP cell surface half-life among cultured primary enterocytes isolated from uninfected ST3Gal6-deficient mice and WT littermates at 8 to 10 weeks of age. (**H** and **I**) In situ localization and intracellular colocalization of IAP in duodenum, depicting the percentage of IAP colocalization (yellow). Graphs are representative of 10 fields of view (n = 4 per genotype). Scale bars, 10 μm. (A to I) *St3Gal6*-deficient mice and WT littermates at 8 to 10 weeks of age, uninfected. (A to D) n = 8 per condition. (E to G) n = 6 per condition. Error bars represent means ± SEM. ***P < 0.001, **P < 0.01, and *P < 0.05; Student's t test (A to G and I).

reduced IAP and the onset of disease symptoms, whereas total LPS increased only modestly in the intestinal contents of infected mice (Fig. 4D). LPS is generated predominantly in the colon by commensal microbes that may serve as markers or effectors of intestinal inflammatory disease (*20*).

A survey of microbiota using 16*S* ribosomal DNA (rDNA) probes revealed a 50% increase of intestinal bacterial load attributed primarily to the Gram-negative Enterobacteriaceae, consistent with the magnitude of increase of total LPS. These findings were present among both uninfected *St3gal6*-null mice and wild-type littermates subjected to recurrent ST infection (Fig. 4E). The temporal acquisition of these microbiota changes observed at 32 weeks was found to emerge progressively among wild-type mice receiving periodic ST infections and was coincident with the emergence and increase in the severity of disease symptoms (fig. S6). These findings are also consistent with reports of altered commensal microbiota populations that can contribute intestinal inflammation and that often include elevated levels of Enterobacteriaceae (*3*, *21*).

ST3Gal6 deficiency spontaneously increased inflammatory cytokines in the intestinal tissues of uninfected animals, and this was further exacerbated by recurrent ST infection (Fig. 4F). Similarly, histopathological findings in the absence of ST3Gal6 correlated with elevated inflammatory marker expression and leukocyte infiltration, epithelial layer discontinuity, and reduced goblet cell numbers, which were also increased in severity by recurrent ST infection (Fig. 4G). These results demonstrated that the ST3Gal6 sialytransferase is essential to support normal IAP sialylation and expression and thereby host protection against spontaneous intestinal inflammation. The cause of IAP desialylation after ST infection was unaccounted for but implicated as a significant trigger of pathogenesis.

Disease onset with neuraminidase induction is TLR4-dependent and recapitulated by LPS

Neuraminidase (Neu) enzymes, also known as sialidases, hydrolyze sialic acids attached to glycan polymers and are encoded in the genomes of diverse organisms, including bacteria, mice, and humans. However, the genome of the ST isolate used in our studies does not encode a Neu (*22*), indicating a host source of the induced Neu activity. Four Neu genes have been identified in mammalian genomes (*Neu1* to *Neu4*), with NEU1 and NEU3 enzymes expressed in multiple compartments, including the cell surface, and in the blood (*23*, *24*). An increase in Neu activity occurred in the small intestine because of ST infection. Studies of Toll-like receptor 4 (*Tlr4*)–null mice revealed that this induction of host Neu activity was dependent on TLR4 function (Fig. 5A). Among mammalian Neu isozymes, only NEU3 abundance and *Neu3* RNA expression correlated with TLR4-dependent induction of Neu activity (Fig. 5, B and C). The absence of *Neu3* induction due to TLR4 deficiency resulted in normal IAP expression at the enterocyte cell surface (Fig. 5D). This was coincident with normal levels of sialic acid linkages on IAP and among apical glycoproteins of the small intestinal epithelium (fig. S5, C and D). AP activity and IAP abundance also remained normal in TLR4 deficiency, and LPS-phosphate levels did not increase significantly after ST infections (Fig. 5, E to G). The induction of inflammatory cytokines caused by recurrent ST infection was also blocked by TLR4 deficiency, and signs of disease were reduced or eliminated with the maintenance of epithelial barrier function (Fig. 5, H and I).

TLR4 is activated by binding to its LPS ligand (*25*, *26*). The LPS bacterial endotoxin is found predominantly in the colon (*27*, *28*), where it can initiate proinflammatory signaling to engage immune

Downloaded from http://science.sciencemag.org/ on December 21, 2017

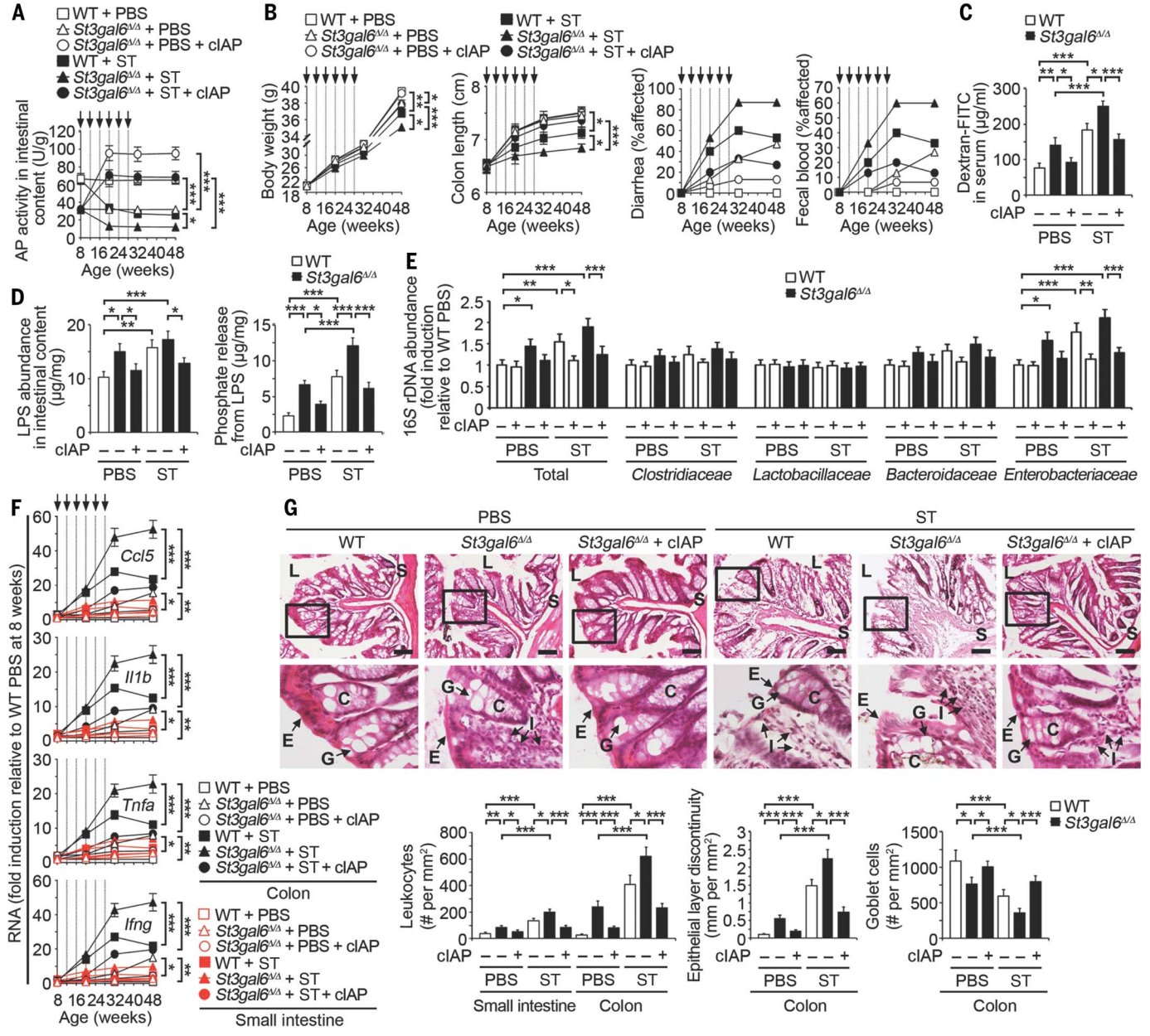


Fig. 4. ST3Gal6 sialylation of IAP prevents intestinal inflammation. Indicated genotypes after ST reinfection (arrows) were analyzed in the absence or presence of cIAP. (**A**) AP activity (n = 32 per condition). (**B**) Body weight (n = 10 per condition), colon length (n = 32 per condition), diarrhea (n = 30 per condition), and fecal blood (n = 30 per condition). (**C**) Intestinal epithelial barrier function. (**D**) LPS abundance and phosphate released from LPS of intestinal content. (**E**) Commensal microbiome 16S rDNA in intestinal content (n = 10 per condition). (**F**) Inflammatory cytokine RNA in colon and small intestine (n = 24 per condition). (**G**) H&E-stained colon sections. Graphs are representative of 10 fields of view (n = 4 per condition). Scale bars, 100 μm. (C and D) Data were acquired from mice 20 weeks of age before fourth infection. (E to G) Data were acquired from mice 32 weeks of age and 4 weeks after the last infection. (C and D) n = 8 per condition. Error bars represent means ± SEM. ***P < 0.001, **P < 0.01, and *P < 0.05; one-way ANOVA with Tukey's multiple comparisons test (A to G).

cells in the onset and development of disease (*29*, *30*). We investigated whether LPS was itself sufficient for Neu induction, IAP deficiency, and concurrent elevations of inflammatory cytokines. Dose-response analyses using commercially obtained LPS were undertaken to determine minimal dosage and timing for further study (fig. S7, A and B). We found that gastric intubation of LPS induced Neu activity, NEU3 abundance, and *Neu3* RNA levels with reductions in AP activity and IAP abundance, all of which were dependent on TLR4 function (Fig. 6, A to F). The induction of Neu activity by LPS resulted in TLR4-dependent reductions of sialic acid linkages with galactose exposure on isolated IAP and among apical cell surface glycoproteins of the small intestinal epithelium (fig. S7, C and D). LPS increased the internalization and colocalization of IAP with endocytic markers coincident with reduced IAP expression at the cell surface (fig. S7E). Normal IAP levels were retained after LPS administration in TLR4 deficiency with relatively low abundance of LPS-phosphate (Fig. 6G). The induction of LPS-induced inflammatory cytokines was also blocked by TLR4 deficiency with the retention of epithelial barrier function (Fig. 6, H and I). Thus, LPS/TLR4 signaling resulting from recurrent low-titer ST infection is linked to the induction of host NEU3 and increased Neu activity, resulting in IAP desialylation and its subsequent

Downloaded from http://science.sciencemag.org/ on December 21, 2017

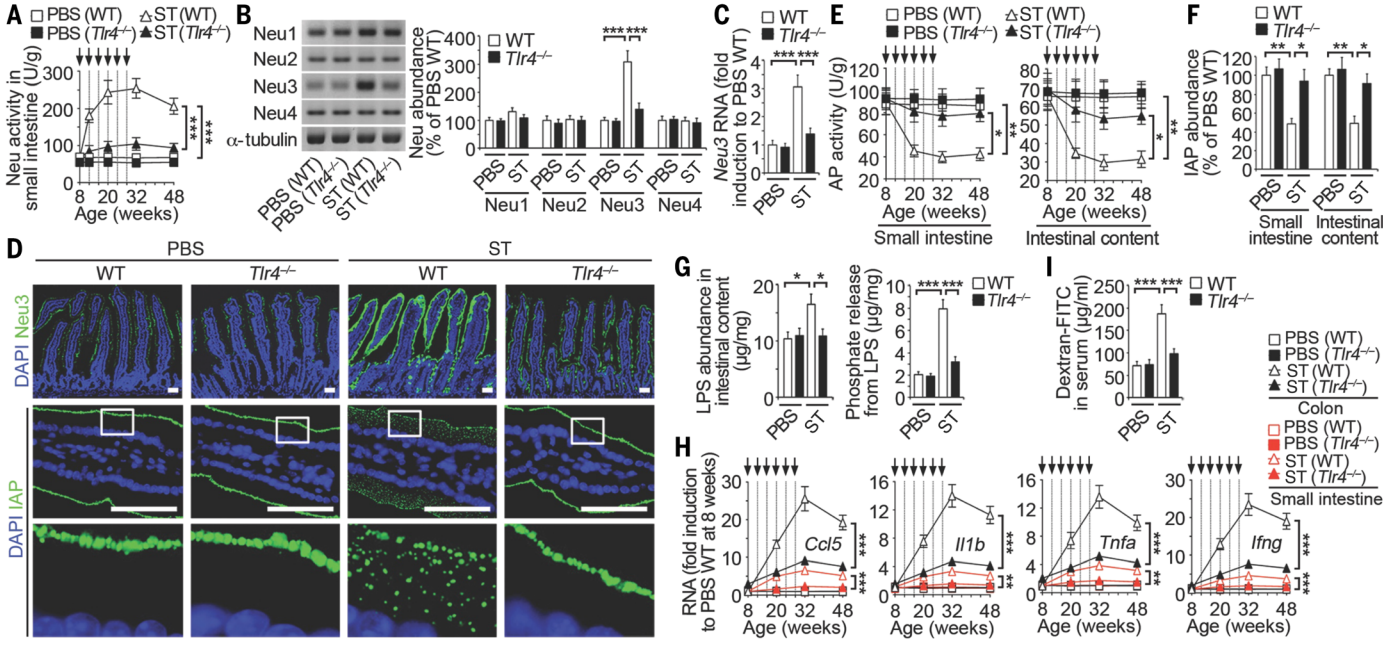


Fig. 5. Host Neu is induced by TLR4 during recurrent ST infection. WT and *Tlr4*-deficient mice were analyzed after recurrent ST infections (arrows). (**A**) Neu activity (n = 30 per condition). (**B**) NEU1 to NEU4 protein abundance in the small intestine. (**C**) *Neu3* mRNA expression in small intestine. (**D**) In situ localization of NEU3 and IAP in duodenum. Images are representative of 10 fields of view (n = 4 per condition). Scale bars, 50 μm. (**E**) AP activity (n = 24 per condition). (**F**) IAP protein abundance. (**G**) LPS abundance and phosphate released from LPS of intestinal content. (**H**) Inflammatory cytokine RNA abundance (n = 16 per condition). (**I**) Intestinal epithelial barrier function. (B, C, F, G, and I) n = 6 per condition. (B, C, F, G, and I) Animals were 20 weeks of age before the fourth infection. Error bars represent means ± SEM. ***P < 0.001, **P < 0.01, and *P < 0.05; one-way ANOVA with Tukey's multiple comparisons test (A to I).

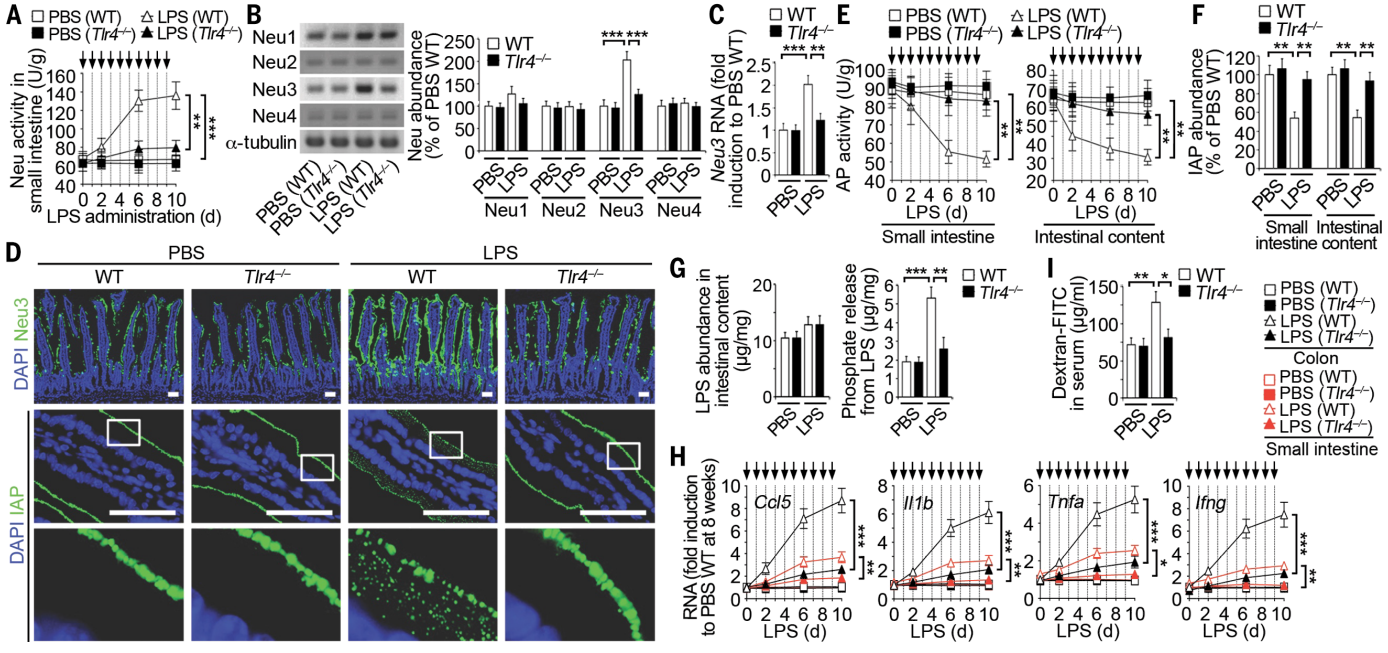


Fig. 6. Host Neu is induced by TLR4 and LPS. (**A**) Neu activity in mice at 8 weeks of age before repeated LPS administrations (arrows). (**B** and **C**) Neu protein abundance and *Neu3* RNA expression in small intestine. (**D**) In situ localization of NEU3 and IAP in duodenum sections, representative of 10 fields of view (n = 4 per condition). Scale bars, 50 μm. (**E**) AP activity before repeated LPS administrations (arrows). (**F**) IAP protein abundance. (**G** to **I**) Phosphate released from LPS of intestinal content, inflammatory cytokine RNA abundance, and intestinal epithelial barrier function. (A and E) n = 24 per condition. (B, C, F, G, and I) n = 6 per condition. (H) n = 16 per condition. (B, C, F, G, and I) Mice on day 6 after LPS administration. Error bars represent means ± SEM. ***P < 0.001, **P < 0.01, and *P < 0.05; one-way ANOVA with Tukey's multiple comparisons test (A to I).

Downloaded from http://science.sciencemag.org/ on December 21, 2017

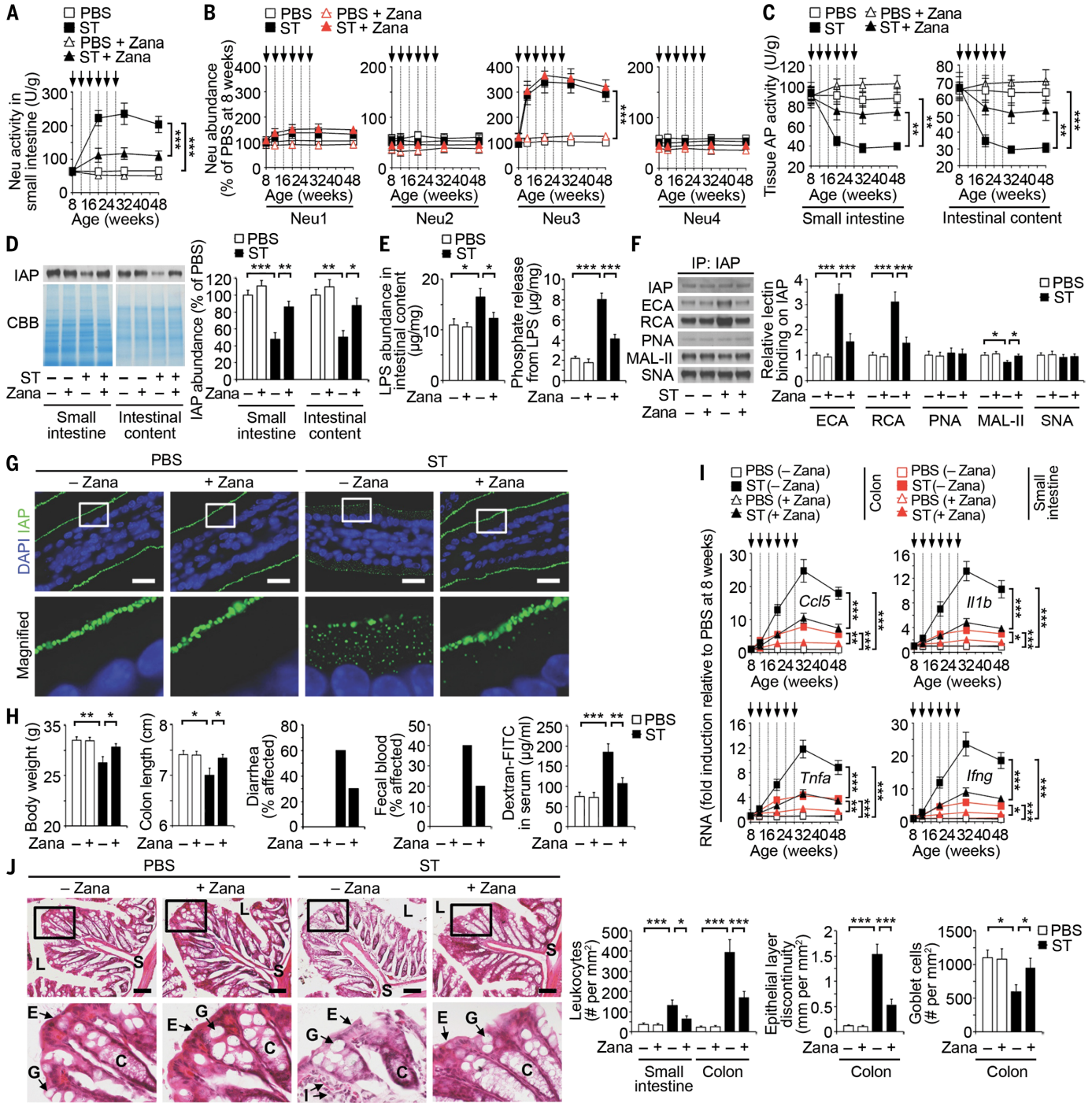


Fig. 7. Effects of the Neu inhibitor zanamivir on intestinal inflammation. WT mice were analyzed at indicated ages before ST reinfection (arrows) in the absence or presence of zanamivir (Zana) (0.5 mg/ml) provided in drinking water immediately after first infection. (**A**) Neu activity. (**B**) NEU1 to NEU4 protein abundance in small intestine. (**C**) AP activity. (**D**) IAP protein abundance. (**E**) LPS abundance and phosphate released from LPS of intestinal content. (**F**) Lectin blotting of IAP protein from small intestine. (**G**) In situ localization of IAP in duodenum, representative of 10 fields of view (n = 4 per condition). Scale bars, 20 μm. (**H**) Body weight (n = 10 per condition), colon length (n = 8 per condition), diarrhea (n = 10 per condition) and fecal blood (n = 10 per condition) at 32 weeks of age, and intestinal epithelial barrier function (n = 8 per condition) at 20 weeks of age. (**I**) Inflammatory cytokine RNA abundance. (**J**) H&E-stained colon sections at 32 weeks of age. Graphs are representative of 10 fields of view (n = 4 mice per condition). Scale bars, 100 μm. (D to G) Mice at 20 weeks of age. (A and C) n = 32 per condition. (B and I) n = 30 per condition. (D to F) n = 6 per condition. Error bars represent means ± SEM. ***P < 0.001, **P < 0.01, and *P < 0.05; one-way ANOVA with Tukey's multiple comparisons test (A to J).

Downloaded from http://science.sciencemag.org/ on December 21, 2017

pathogenic deficiency. Thus, Neu inhibition may be therapeutic in the context of recurrent ST infection.

Therapeutic effect of zanamivir entails the maintenance of IAP abundance and function

The marketed antiviral drug zanamivir inhibits influenza Neu activity (*31*) and has been used in research on mammalian Neu isozymes (*24*, *32*, *33*). At pharmacological dosages, zanamivir inhibits NEU2, NEU3, and NEU4 but not NEU1 (*32*, *33*). We found that oral treatment with zanamivir maintained normal Neu activity levels in animals experiencing recurrent ST infections (Fig. 7A). Zanamivir did not block the physical induction of NEU3, which persisted for at least 20 weeks after the last ST infection (Fig. 7B). However, the inhibition of Neu activity by zanamivir maintained host AP activity, IAP abundance, and normal lectin-binding patterns among apical glycoproteins of the small intestinal epithelium (Fig. 7, C and D, and fig. S8). The maintenance of IAP expression and activity was linked to the retention of relatively low LPS-phosphate levels that were otherwise elevated by ST infection (Fig. 7E). Zanamivir inhibited IAP desialylation coincident with normal IAP expression at the enterocyte cell surface (Fig. 7, F and G). Zanamivir also inhibited the induction of inflammatory cytokines and reduced the appearance of disease markers of intestinal inflammation, including alterations of commensal microbiota and barrier dysfunction (Fig. 7, H to J, and fig. S9). In contrast, for acute and chronic models of chemically induced colitis using dextran sodium sulfate (DSS) (*34*, *35*), zanamivir had no effect, whereas ST3Gal6 deficiency exacerbated signs of disease, consistent with the presence of different inflammatory mechanisms that may be responsive to IAP treatment (fig. S10). Our findings together indicate a disease mechanism of environmental and pathogen origin, which encompasses the different locations and functions of the small intestine and colon (Fig. 8).

Discussion

An increasingly severe colitis developed from recurrent low-titer nonlethal transient gastric infections of the Gram-negative pathogen ST. In this mouse model of repeated human food poisoning, the host rapidly cleared the pathogen. Nevertheless, subsequent recurrent infections progressively disabled a mechanism in the host that normally protects against spontaneous intestinal inflammation. This anti-inflammatory mechanism operates primarily in the colon but is dependent on IAP production and release from duodenal enterocytes of the small intestine. ST infection targeted this protective mechanism by activating host TLR4 function in the duodenum, inducing host Neu activity with elevated NEU3 expression at the luminal surface of the enterocyte. Neu induction accelerated the rate of nascent IAP aging by desialylation on the enterocyte cell surface, reducing IAP half-life, inducing IAP internalization and degradation, and resulting in a downstream IAP deficiency in the colon. IAP deficiency was linked to the deficient dephosphorylation of LPS molecules produced by commensal microbiota. This TLR4-dependent disease manifested primarily in the colon with IBD-like symptoms closer to UC than Crohn's disease, and was linked to increases in the proinflammatory TLR4 ligand LPS-phosphate. Similarly, the genetic disruption of ST3Gal6-dependent sialic acid linkage formation during IAP synthesis caused IAP deficiency, resulting in a spontaneous colitis, which increased in severity with age and was exacerbated by recurrent ST infections. In both cases, diminished glycoprotein sialylation among enterocytes resulted in reduced IAP half-life, leading to IAP deficiency with markedly elevated LPS-phosphate abundance in the colon. Consistent with a TLR4-dependent mechanism, LPS administration alone recapitulated NEU3 induction and IAP deficiency, bypassing the requirement for IAP deficiency to increase colonic LPS-phosphate levels in provoking inflammation.

Intestinal inflammation failed to resolve after the discontinuation of periodic recurrent infections and persisted for months afterward as a lasting outcome. The degree of this persistence may be determined in part by initial infection titers and the time between recurrent infections and may result from multiple mechanisms. One possibility is the generation of epigenetic modifications to inflammatory gene promoters regulated by TLR4 function that result in the persistence of inflammatory cytokine expression, and may explain observations of the slow resolution of inflammatory processes (*36*, *37*). The enterocyte *Neu3* allele is perhaps regulated in this way because its expression remained induced long after periodic ST infections were discontinued. It is also possible that the escalating inflammation resulting from increased recruitment and activation of innate and adaptive immune cells reaches a point wherein the degree of immunological activation and damage to the epithelium is not easily reversed or attenuated. Disease persistence was also coincident with microbiota alterations that we found emerged concurrently with signs of disease and endured after the discontinuation of recurrent infections. In this regard, acute enteric infections with *Yersinia* can trigger gut microbiota dysbiosis and chronic inflammation after pathogen clearance in *Tlr1*-deficient mice (*38*). In addition, the microbiota alterations that we observed predominantly involved Enterobacteriaceae, which are frequently imbalanced in studies of intestinal inflammatory disease (*21*, *38*).

Neu enzymes function in a variety of processes, including pathogen virulence, glycan catabolism, and biological signaling (*39*–*41*) and may differ among isozymes and origins, such as indicated from cecal sources in contributing to DSS-induced colitis (*34*). Mammalian *Neu3* includes presumptive binding sites for transcriptional factors STAT3, RREB1, MYOD, Ik2, PAX2, Aml1a, HOXA9, and MEIS1 and may use alternate promoters controlled by Sp1/Sp3 transcription factors (*42*). Indeed, STAT3 and Sp1 transcription factors are

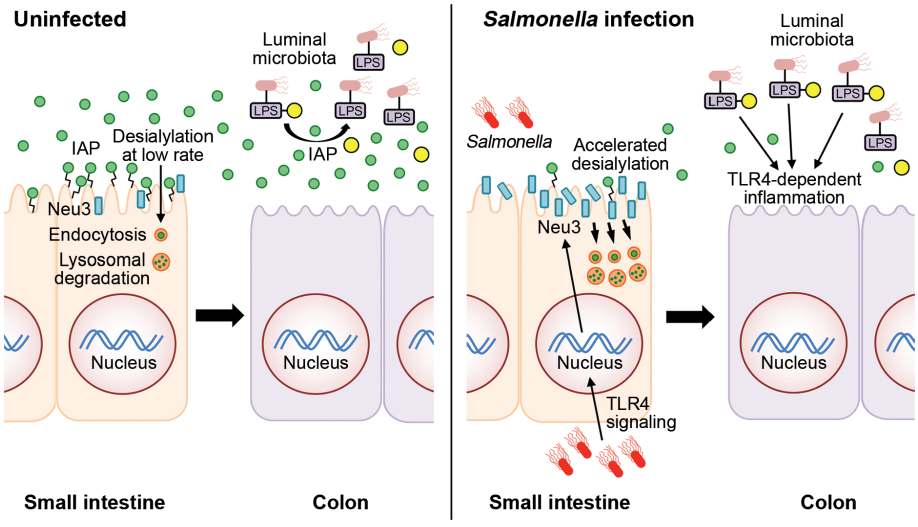


Fig. 8. Model of intestinal inflammation due to recurrent Gram-negative ST infection. In the absence of infection of the small intestine, the anti-inflammatory GPI-linked IAP glycoprotein (green circles) is highly expressed on the enterocyte cell surface. IAP is eventually released into the lumen and travels through the intestinal tract to the colon where it detoxifies LPS-phosphate produced by Gram-negative and commensal bacteria via dephosphorylation (yellow circles). Nascent IAP at the enterocyte cell surface undergoes a low rate of desialylation linked to the rate of internalization and degradation involving a normal mechanism of IAP aging and turnover. Enterocytes of the small intestine respond to LPS-phosphate and ST infection by activating TLR4 function, which induces host NEU3 Neu (blue bars) on the enterocyte surface. Increased Neu activity accelerates the rate of IAP desialylation and internalization (orange circles), reducing IAP abundance and resulting in increased levels of LPS-phosphate in the colon where TLR4 activation elicits inflammation and disease.

Downloaded from http://science.sciencemag.org/ on December 21, 2017

activated by LPS (43, 44). The transcriptional activation of *Neu3* may further underlie NEU3 induction in cancers of colon, renal, and prostate tissues, whereas mice lacking NEU3 exhibited fewer colitis-associated colonic tumors (45–47). Our studies of an ST isolate lacking an annotated and demonstrable Neu gene have further linked *Neu3* RNA induction with the elevation of host Neu activity, supporting the view that host NEU3 is involved in the desialylation of the IAP glycoprotein, which results in IAP internalization and deficiency. However, it remains possible that the Neu activity that we have measured comes from an unannotated Neu enzyme or the endogenous microbiota, neither of which can be resolved until *Neu3*-deficient mice are further studied. Although NEU3 activity is primarily active toward gangliosides, studies have shown significant but lesser activity toward glycoprotein substrates (48). It is also possible that NEU3 may act indirectly via the desialylation of its canonical ganglioside substrates. Nevertheless, NEU3 has been reported to desialylate the epidermal growth factor receptor glycoprotein (49). Moreover, data similar to our present findings have further implicated NEU3 in the desialylation of circulating glycoproteins in the blood linked to a mechanism that determines the various half-lives of plasma proteins (24).

The regulation of enterocyte IAP trafficking by sialylation extends this recently discovered mechanism of secreted protein aging and turnover to include the determination of protein half-lives at the cell surface. Although ST infection resulted in the desialylation and internalization of multiple enterocyte glycoproteins expressed at the cell surface, the disease phenotype was largely due to IAP deficiency. This represents an example of a specific glycan linkage that is commonly found on secreted and cell surface proteins having a biological purpose more restrictively associated with one or a few such glycoproteins (50–52). This can be explained, in part, by the presence of multiple sialyltransferases operating in the intestinal tract, which are responsible for the sialylation of different subsets of bioactive glycoproteins and which function in different biological processes. For example, the present findings involving ST3Gal6 deficiency should be compared with other studies of ST3Gal4 deficiency (34). Additional factors that may influence IAP expression and disease onset include mutations of glycan acceptor sites of IAP and transcriptional or mutagenic modifications to relevant glycosyltransferase and glycosidase genes, each of which can contribute to glycoprotein function (53). The control of IAP half-life via the increased internalization and degradation of desialylated IAP implies the possible presence of a sialic acid–binding lectin analogous to the mammalian siglecs of leukocytes (54). Such lectins may normally bind nascent sialylated IAP on the enterocyte surface to inhibit premature IAP endocytosis, enabling the subsequent release of IAP into the lumen. Alternatively, the exposure of underlying galactose may unmask cryptic ligands for galactose-binding lectins, such as the galectins, which modulate glycoprotein endocytosis (50, 55).

Diminished AP activity has been described in patients with colitis and celiac disease, and oral AP supplementation is under investigation for the treatment of inflammatory diseases, including the IBDs (56–59). Moreover, NEU3 protein abundance and activity is reportedly increased in human IBD patients (60). In animal studies, IAP deficiency contributes to colitis and allows increased bacterial transit from the intestinal lumen to the mesenteric lymph nodes (16, 35, 56, 61). We have found that IAP is highly regulated and that ST infection disables IAP function in host protection while progressively eroding microbial barriers by successive rounds of what might otherwise be considered unproductive infections. Environmental Gram-negative pathogens that access and infect the small intestine may have a similar strategy toward misappropriating host TLR4 function to diminish IAP activity and increase colonic LPS-phosphate levels, provoking intestinal inflammation. This further emphasizes the dual nature of host TLR4 function, which may be either advantageous or disadvantageous perhaps depending on the context of exposure and the severity of infection. Although the link that we identified between host TLR4 function and NEU3 induction appears to favor the pathogen, advantageous features of TLR4 signaling may become evident with high *Salmonella* titers that engender extended pathogen colonization of the intestinal tract. Nevertheless, IAP augmentation and Neu inhibition represent candidate therapies for preventing the onset and progression of an escalating colitis that originates from recurrent low-titer *Salmonella* infections, as may occur in common cases of human food poisoning.

Materials and methods

Laboratory animals

Inbred C57BL/6J mice were used (Jackson Laboratory). *St3gal6*-deficient mice (19) were backcrossed six or more generations into the C57BL/6J background prior to study. *TLR4*$^{-/-}$ mice (B6(Cg)-Tlr4$^{tm1.2Karp}$/J) were purchased from the Jackson Laboratory. Littermates bearing normal alleles were used as controls. All mice analyzed were provided sterile pellet food and water ad libitum. Institutional Animal Care and Use Committees of the University of California Santa Barbara and the Sanford Burnham Prebys Medical Discovery Institute approved studies undertaken herein.

Bacterial strains and infection protocols

Salmonella enterica subsp. *enterica* serovar Typhimurium reference strain ATCC 14028 (CDC 6516-60) was used as previously described (62). For the induction of chronic colitis, 8-week-old mice were infected with *ST* (2×10^3 cfu) via gastric intubation up to five times at 4-week intervals after the initial infection. For monitoring the development of colitis, mice were weighed biweekly and assessed for colitis-associated symptoms, including the presence of diarrhea, stool consistency (0, normal; 2, loose stools; 4, diarrhea), fecal blood (occult fecal blood positive, Beckman Coulter), and rectal prolapse as previously described (63).

Histology

Mouse tissues were fixed in 10% buffered formalin (Sigma-Aldrich), transferred to 30% sucrose/PBS, and embedded in Tissue-Tek OCT compound (Sakura Finetek). Three-micron frozen serial sections were stained with hematoxylin and eosin (H & E; Sigma-Aldrich) or incubated with 1 μg/ml of antibodies to one or more molecules including CD3ε (M-20, Santa Cruz Biotechnology), Gr-1 (M-66, Santa Cruz Biotechnology), F4/80 (M-300, Santa Cruz Biotechnology), TNFα (M-18, Santa Cruz Biotechnology), EEA1 (C-15, Santa Cruz Biotechnology), LAMP2 (C-20, Santa Cruz Biotechnology), γ-adaptin (I-19, Santa Cruz Biotechnology), Calnuc (V-18, Santa Cruz Biotechnology), protein disulfide isomerase PDI (G-20, Santa Cruz Biotechnology), Neu3 (M-50, Santa Cruz Biotechnology), sucrase-isomaltase (A-17, Santa Cruz Biotechnology), dipeptidyl peptidase 4 (H-270, Santa Cruz Biotechnology), lactase (T-14, Santa Cruz Biotechnology), or 1:1000 dilution of IAP specific antiserum kindly provided by Dr. Jose Millan (64), or 5 μg/ml of biotinylated lectins including *Erythrina cristagalli* (ECA), *Ricinus Communis* Agglutinin-I (RCA), Peanut Agglutinin (PNA), *Maackia amurensis*-II (MAL-II), or *Sambucus nigra* (SNA) (Vector Laboratories). CD3ε, TNFα, sucrase-isomaltase, and lactase were visualized with 0.4 μg/ml of FITC-conjugated rabbit anti-goat IgG (Santa Cruz Biotechnology); Gr-1, F4/80, IAP, Neu3, and dipeptidyl peptidase 4 were visualized with FITC-conjugated goat 0.4 μg/ml of anti-rabbit IgG (Santa Cruz Biotechnology); EEA1, LAMP2, γ-adaptin, Calnuc, and PDI were visualized with 0.4 μg/ml of Texas Red-conjugated rabbit anti-goat IgG (Santa Cruz Biotechnology) and biotinylated lectins were visualized with 1 μg/ml of FITC-conjugated streptavidin (Vector Laboratories). These primary antibody or lectin incubations were performed at 4°C overnight and secondary antibody or streptavidin incubations were performed at room temperature for 1 h. All microscopic work was performed using a TissueGnostics microscopy workstation equipped with Zeiss AxioImager Z1 microscope system, Hamamatsu C13440-20C camera, PixeLINK PL-D673CU camera, and Lumen Dynamics X-Cite XLED1 illuminator. All microscopic images were obtained and histopathological studies including quantification of cells, cell boundaries, and marker expression were performed with TissueFAXS (Version 3.5), TissueQuest (Version 4.0), and HistoQuest software (Version 4.0) (TissueGnostics USA Ltd.). Colocalization was further quantified by MetaMorph software (Version 7.0) (Universal Imaging Corporation) (65). Yellow signals in merged images of IAP (green) and intracellular compartments (red) indicate colocalization, and the threshold intensity value of 12 (intensity range, 0–255) and size of 0.026 μm^2 were used as the cut-off.

mRNA preparation and quantification by real-time PCR

Total RNA was isolated from tissues using Trizol (Invitrogen) and subjected to reverse transcription (RT) using SuperScript III (Invitrogen). Quantitative real-time PCR was performed using Brilliant SYBR Green Reagents with the Mx3000P

Downloaded from http://science.sciencemag.org/ on December 21, 2017

QPCR System (Stratagene). Primers used for real-time PCR in the mouse were: CCL5-RT-F (5′-TCGTGTTTGTCACTCGAAGG-3′), CCL5-RT-R (5′-CTAGCTCATCTCCAAATAGT-3′), IL-1b-RT-F (5′-GCCCATCCTCTGTGACTCAT-3′), IL-1b-RT-R (5′-AGGCCACAGGTATTTTGTCG-3′), TNFa-RT-F (5′-CATCTTCTCAAAATTCGAGT-3′), TNFa-RT-R (5′-TTTGAGATCCATGCCGTTGG-3′), IFNg-RT-F (5′-ACTGGCAAAAGGATGGTGAC-3′), IFNg-RT-R (5′-GTTGCTGATGGCCTGATTGT-3′), Neu3-RT-F (5′-CTCAGTCAGAGATGAGGATGCT-3′), Neu3-RT-R (5′-GTGAGACATAGTAGGCATAGGC-3′), IAP-RT-F (5′- CTCATCTCCAACATGGAC-3′), IAP-RT-R (5′-TGCTTAGCACTTTCACGG-3′), GAPDH-RT-F (5′-TGGTGAAGGTCGGTGTGAAC-3′) and GAPDH-RT-R (5′-AGTGATGGCATGGACTGTGG-3′). Relative mRNA levels were normalized to expression of GAPDH RNA.

Immunoprecipitation, immunoblotting, and lectin blotting

Tissue samples were homogenized in radioimmunoprecipitation assay (RIPA) buffer (50 mM Tris-HCl (pH 7.6), 150 mM NaCl, 1 mM EDTA, 1% NP-40, 1% sodium deoxycholate, and 0.1% SDS) supplemented with complete protease inhibitor cocktail per instructions (Roche) and incubated overnight at 4°C on a rotating wheel with 1:100 dilution of IAP-specific antiserum (*64*) or 2 μg/ml of antibodies to sucrase-isomaltase (A-17, Santa Cruz Biotechnology), dipeptidyl peptidase 4 (H-270, Santa Cruz Biotechnology), or lactase (T-14, Santa Cruz Biotechnology), followed by 2 h of incubation in the presence of protein A/G PLUS agarose (Santa Cruz Biotechnology). Immunoprecipitates were washed five times with RIPA buffer and eluted with SDS sample buffer. Protein samples eluted were subjected to SDS-PAGE, transferred to nitrocellulose membranes and incubated with 2% BSA in Tris-buffered saline (TBS). They were then analyzed by immunoblotting using either 1 μg/ml of antibodies to Neu1 (H-300, Santa Cruz Biotechnology), Neu2 (M-13, Santa Cruz Biotechnology), Neu3 (M-50, Santa Cruz Biotechnology), Neu4 (N-14, Santa Cruz Biotechnology), sucrase-isomaltase (A-17, Santa Cruz Biotechnology), dipeptidyl peptidase 4 (H-270, Santa Cruz Biotechnology), lactase (T-14, Santa Cruz Biotechnology), α-Tubulin (H-300, Santa Cruz Biotechnology), or 1:1000 dilution of anti-IAP antiserum, or by lectin blotting with HRP-conjugated ECA (0.5 μg/ml), RCA (0.1 μg/ml), PNA (1 μg/ml), MAL-II (0.2 μg/ml), or SNA (0.1 μg/ml) (EY Laboratories). Signals detected by chemiluminescence (GE Healthcare) were analyzed by integrated optical density using Labworks software (UVP Bioimaging Systems). Parallel protein samples were visualized with Coomassie brilliant blue G250 staining (Bio-Rad).

Neuraminidase activity and inhibition

Neuraminidase activity was measured in tissue extracts in RIPA buffer using the Amplex Red Neuraminidase Assay Kit according to the manufacturers' instructions (Molecular Probes). For inhibition of neuraminidase activity in the small intestine and colon, zanamivir (0.5 mg/ml; Sigma-Aldrich) was provided in the drinking water immediately following the initial *ST* infection at 8 weeks of age, and continued for the duration of study as indicated.

ELISA

Enzyme-linked immunosorbent assay (ELISA) plates (Nunc) were coated with 2 μg/ml of antibodies to either Neu1 (H-300, Santa Cruz Biotechnology), Neu2 (M-13, Santa Cruz Biotechnology), Neu3 (M-50, Santa Cruz Biotechnology), Neu4 (N-14, Santa Cruz Biotechnology), sucrase-isomaltase (A-17, Santa Cruz Biotechnology), dipeptidyl peptidase 4 (H-270, Santa Cruz Biotechnology), or lactase (T-14, Santa Cruz Biotechnology), or 1:1000 dilution of IAP antiserum, and blocked with BSA before incubation with serial dilutions of mouse tissue extracts that were biotinylated using 1 mg/ml of N-hydroxysuccinimide-biotin (Pierce). Antigens were detected following the addition of 1:1000 dilution of HRP-streptavidin (BD Biosciences) and 3,3′,5,5′ tetramethylbenzidine (TMB, Sigma-Aldrich). Lectin binding was determined in parallel by the addition of HRP-conjugated ECA (0.5 μg/ml), RCA (0.1 μg/ml), PNA (1 μg/ml), MAL-II (0.2 μg/ml), or SNA (0.1 μg/ml) (EY Laboratories), followed by TMB, and changes in glycan linkages were detected by comparing lectin binding among identical amounts of biotinylated IAP, sucrase-isomaltase, dipeptidyl peptidase 4, or lactase antigen calculated as described (*66*). Alkaline phosphatase activity was measured using the *p*-nitrophenyl phosphate substrate (pNPP; Sigma-Aldrich) as previously described (*61*).

LPS phosphorylation

To determine LPS content in the intestinal contents, LPS was isolated as previously described (*67*) by the hot phenol–water method with minor modifications. Briefly, the intestinal contents were weighed, diluted ten-fold weight to volume in Tris-buffered saline (TBS), and homogenized. The extract solution of intestinal contents was added to same volume of 99% phenol (Ambion), preheated to 65°C and incubated for 15 min at 65°C. After cooling on ice, the samples were centrifuged at 10,000 × *g* for 10 min. The aqueous phase was acquired and residual phenol was removed by extracting with diethyl ether (Sigma-Aldrich). The diethyl ether phase was discarded and the water phase containing the LPS was placed in a hood for 1 h to allow the remaining diethyl ether to evaporate. The above steps were repeated after treatment with proteinase K (Promega), RNase (Invitrogen) and DNase (Invitrogen). LPS preparations from indicated sources were quantified by the purpald assay as described previously (*68*). LPS preparations for comparative studies were indistinguishable by chromatography and silver staining (Bio-Rad). To compare the abundance of phosphate linked to LPS, phosphate release was measured by the malachite green phosphate assay (*61*). Briefly, purified calf intestinal alkaline phosphatase (10 U; Invitrogen) was incubated at pH 8.0 for 3 h at 37°C with 1 mg of LPS isolated from intestinal contents. Free phosphate released was measured as a colored complex of phosphomolybdate and malachite green at 620 nm according to the manufacturer's instructions (BioAssay Systems).

Pulse–chase analysis and cell-surface half-life

Techniques as previously described (*50*) were used for pulse–chase measurements of IAP synthesis and trafficking among cultured primary enterocytes. Mouse enterocytes were isolated from the duodenum as previously described (*69*). The proximal duodenum was removed and flushed through with solution A (1.5 mM KCl, 96 mM NaCl, 27 mM sodium citrate, 8 mM KH_2PO_4, 5.6 mM Na_2HPO_4) at room temperature. The duodenum was minced in an enzyme cocktail (333 U/ml collagenase, 2.5 U/ml elastase, and 10 μg/ml DNAse) in HEPES-buffered Krebs Ringer solution (5 mM HEPES (4-(2-hydroxyethyl)-1-piperazineethanesulfonic acid, pH 7.4), 120 mM NaCl, 24 mM $NaHCO_3$, 4.8 mM KCl, 1.2 mM $MgSO_4$, 1.2 mM KH_2PO_4, 20 mM glucose, 1 mM $CaCl_2$) and incubated while shaking at 37°C for 30 minutes. Cells were filtered through a 70-μm filter and washed twice in Dulbecco's modified Eagle's medium (DMEM) supplemented with 10% fetal calf serum, 1% β-mercaptoethanol, and 1% L-asparagine. Isolated enterocytes were washed twice with Hank's balanced salt solution (HBSS), then incubated with DMEM depleted of methionine (Gibco) with 10% fetal calf serum for 2 h at 37°C. Pulse labeling was performed with 400 μCi/ml [^{35}S]methionine for 10 min at 37°C, and cells were then washed twice in ice-cold HBSS. Cells were lysed or returned to new media of above culture conditions containing 2 mM methionine for 15, 30, 45, 60, or 90 min. Media used in chase samples were harvested at each time point. Cells used in chase samples were washed twice with ice-cold PBS and incubated with 1 mg/ml of sulfo-NHS-LC-biotin (Pierce Chemical) at 4°C for 30 min. Biotinylation was stopped by three washes with 15 mM glycine in ice-cold PBS. Cells were homogenized in RIPA buffer, and biotinylated proteins were purified using immobilized monomeric avidin gel (Pierce). Eluates isolated in the presence of D-biotin (Pierce) or media samples for chase were incubated with IAP-specific antiserum. Immunoprecipitates were subjected to SDS-PAGE, and gels were fixed before drying and autoradiography at −70°C for 3–7 days. For cell-surface half-life analysis, primary enterocytes were washed twice with ice-cold PBS and biotinylated with sulfo-NHS-LC-biotin as described above. Cells were further cultured at the indicated times, and then homogenized in RIPA buffer, followed by immunoprecipitation using the IAP-specific antiserum. IAP immunoprecipitates were subjected to SDS-PAGE, transferred to nitrocellulose membranes, and visualized with HRP-conjugated streptavidin. To determine IAP glycosylation on enterocyte surface, primary enterocytes were washed twice with ice-cold PBS and biotinylated with sulfo-NHS-LC-biotin as described above. Cells were further cultured at the indicated times, and then homogenized in RIPA buffer. Biotinylated proteins were purified

Downloaded from http://science.sciencemag.org/ on December 21, 2017

using immobilized monomeric avidin gel and incubated on ELISA plates (Nunc) coated with IAP antiserum. Lectin binding was determined in parallel by the addition of HRP-conjugated ECA, RCA, PNA, MAL-II or SNA, followed by TMB, and changes in glycan linkages were detected by comparing lectin binding among identical amounts of biotinylated IAP antigen calculated as described (*66*).

Calf intestinal alkaline phosphatase (cIAP) treatment and LPS administration

cIAP (20 U/ml; Lee Biosolutions) was provided immediately in drinking water from the time of the initial *ST* infection. For LPS administration, 8-week-old mice were orally administered LPS (100 mg/kg; *E. coli* 0111:B4) via gastrointubation and challenged at 24-h intervals after the initial administration of 10 days.

In vivo intestinal barrier function

Dextran-FITC (Sigma) was administered via oral gavage (600 mg/kg), blood was collected from anesthetized animals into Microtainer Serum Separator Tubes (BD Biosciences) at 4 h with no anticoagulant, and allowed to clot for 30 minutes at room temperature. Serum was collected after centrifugation at 10,000 × *g* for 10 min. The amount of FITC in each sample was measured by using a Spectra Max Gemini EM fluorescent plate reader (Molecular Devices) at 490 and 530 nm for the excitation and emission wavelengths, respectively.

Comparative studies of intestinal microbiota

DNA from intestinal content was isolated with a QIAamp DNA Mini Kit according to the manufacturer's instructions (Qiagen). Commensal microbiota was analyzed by quantitative real-time PCR using Brilliant SYBR Green Reagents with the Mx3000P QPCR System (Stratagene) with specific primers for bacteria (*70*) (Total-F-5′-GTGCCAGCMGCCGCGGTAA-3′, Total-R-5′-GACTACCAGGGTATCTAAT-3′; Clostridiaceae-F-5′-TTAACACAATAAGTWATCCACCTGG-3′, Clostridiaceae -R-5′-ACCTTCCTCCGTTTTGTCAAC-3′; Lactobacillaceae-F-5′-AGCAGTAGGGAATCTTCC-3′, Lactobacillaceae-R-5′-CGCCACTGGTGTTCYTCCATATA-3′; Bacteroidaceae-F-5′-CCAATGTGGGGGACCTTC-3′, Bacteroidaceae-R-5′-AACGCTAGCTACAGGCTT-3′; Enterobacteriaceae-F-5′-CATTGACGTTACCCGCAGAAGAAGC-3′, Enterobacteriaceae-R-5′-CTCTACGAGACTCAAGCTTGC-3′). Relative bacterial DNA levels were related to the amount of total isolated DNA from intestinal content.

DSS-induced acute and chronic colitis

For survival studies in acute colitis, 12-week-old mice were administered drinking water containing 4% dextran sodium sulfate (DSS; molecular weight, 40,000 to 50,000; USB Corp.) ad libitum for 5 days and then returned to normal drinking water without DSS until the end of the experiment (day 14). For other experiments in acute colitis, mice were administered 2% DSS solution in drinking water for 5 days. DSS-induced chronic colitis was induced as previously described (*35*). Briefly, 12-week-old mice were administered 2% DSS solution in drinking water with four cycles of DSS given ad libitum for 7 days followed by a 7-day DSS-free interval. Zanamivir (0.5 mg/ml; Sigma-Aldrich) was provided in the drinking water immediately following the administration of DSS and continued for the duration of study as indicated. Body weight, stool consistency, and the presence of occult blood were determined. Stool scores were determined as follows: 0, well-formed pellets; 1, semiformed stools that did not adhere to the anus; 2, semiformed stools that adhered to the anus; 3, liquid stools that adhered to the anus. Bleeding scores were determined as follows: 0, no blood as tested with hemoccult (Beckman Coulter); 1, positive hemoccult; 2, blood traces in stool visible; 3, gross rectal bleeding as previously described (*71*).

Statistical analysis

All data were analyzed as mean ± SEM unless otherwise indicated. Student's unpaired *t* test, one-way ANOVA with Tukey's multiple comparisons test, log-rank test, or Kruskal-Wallis test with Dunn's multiple comparisons test with GraphPad Prism software (Version 7.0) were used to determine statistical significance among multiple studies. *P* values of less than 0.05 were considered significant. Statistical significance was denoted by $*P < 0.05$, $**P < 0.01$, or $***P < 0.001$.

REFERENCES AND NOTES

1. B. Khor, A. Gardet, R. J. Xavier, Genetics and pathogenesis of inflammatory bowel disease. *Nature* **474**, 307–317 (2011). doi: 10.1038/nature10209; pmid: 21677747
2. A. Kaser, S. Zeissig, R. S. Blumberg, Inflammatory bowel disease. *Annu. Rev. Immunol.* **28**, 573–621 (2010). doi: 10.1146/annurev-immunol-030409-101225; pmid: 20192811
3. P. J. Sansonetti, War and peace at mucosal surfaces. *Nat. Rev. Immunol.* **4**, 953–964 (2004). doi: 10.1038/nri1499; pmid: 15573130
4. D. Knights, K. G. Lassen, R. J. Xavier, Advances in inflammatory bowel disease pathogenesis: Linking host genetics and the microbiome. *Gut* **62**, 1505–1510 (2013). doi: 10.1136/gutjnl-2012-303954; pmid: 24037875
5. J. Halfvarson, Genetics in twins with Crohn's disease: Less pronounced than previously believed? *Inflamm. Bowel Dis.* **17**, 6–12 (2011). doi: 10.1002/ibd.21295; pmid: 20848478
6. L. Eckmann, Animal models of inflammatory bowel disease: Lessons from enteric infections. *Ann. N. Y. Acad. Sci.* **1072**, 28–38 (2006). doi: 10.1196/annals.1326.008; pmid: 17057188
7. A. Sonnenberg, Seasonal variation of enteric infections and inflammatory bowel disease. *Inflamm. Bowel Dis.* **14**, 955–959 (2008). doi: 10.1002/ibd.20408; pmid: 18302273
8. Centers for Disease Control and Prevention (CDC), Vital signs: Incidence and trends of infection with pathogens transmitted commonly through food—Foodborne Diseases Active Surveillance Network, 10 U.S. sites, 1996–2010. *MMWR Morb. Mortal. Wkly. Rep.* **60**, 749–755 (2011). pmid: 21659984
9. E. Scallan *et al.*, Foodborne illness acquired in the United States—Major pathogens. *Emerg. Infect. Dis.* **17**, 7–15 (2011). doi: 10.3201/eid1701.P11101; pmid: 21192848
10. S. E. Majowicz *et al.*,The global burden of nontyphoidal *Salmonella* gastroenteritis. *Clin. Infect. Dis.* **50**, 882–889 (2010). doi: 10.1086/650733; pmid: 20158401
11. H. K. de Jong, C. M. Parry, T. van der Poll, W. J. Wiersinga, Host-pathogen interaction in invasive Salmonellosis. *PLOS Pathog.* **10**, e1002933 (2012). doi: 10.1371/journal.ppat.1002933; pmid: 23055923
12. N. A. Feasey, G. Dougan, R. A. Kingsley, R. S. Heyderman, M. A. Gordon, Invasive non-typhoidal salmonella disease: An emerging and neglected tropical disease in Africa. *Lancet* **379**, 2489–2499 (2012). doi: 10.1016/S0140-6736(11)61752-2; pmid: 22587967
13. B. F. Hinnebusch *et al.*, Enterocyte differentiation marker intestinal alkaline phosphatase is a target gene of the gut-enriched Krüppel-like factor. *Am. J. Physiol. Gastrointest. Liver Physiol.* **286**, G23–G30 (2004). doi: 10.1152/ajpgi.00203.2003; pmid: 12919939
14. K. Poelstra, W. W. Bakker, P. A. Klok, M. J. Hardonk, D. K. Meijer, A physiologic function for alkaline phosphatase: Endotoxin detoxification. *Lab. Invest.* **76**, 319–327 (1997). pmid: 9121115
15. I. Koyama, T. Matsunaga, T. Harada, S. Hokari, T. Komoda, Alkaline phosphatases reduce toxicity of lipopolysaccharides *in vivo* and *in vitro* through dephosphorylation. *Clin. Biochem.* **35**, 455–461 (2002). doi: 10.1016/S0009-9120(02)00330-2; pmid: 12413606
16. J. M. Bates, J. Akerlund, E. Mittge, K. Guillemin, Intestinal alkaline phosphatase detoxifies lipopolysaccharide and prevents inflammation in zebrafish in response to the gut microbiota. *Cell Host Microbe* **2**, 371–382 (2007). doi: 10.1016/j.chom.2007.10.010; pmid: 18078689
17. N. L. Sussman *et al.*, Intestinal alkaline phosphatase is secreted bidirectionally from villous enterocytes. *Am. J. Physiol.* **257**, G14–G23 (1989). pmid: 2546440
18. L. G. Ellies *et al.*, Sialyltransferase specificity in selectin ligand formation. *Blood* **100**, 3618–3625 (2002). doi: 10.1182/blood-2002-04-1007; pmid: 12393657
19. W. H. Yang, C. Nussbaum, P. K. Grewal, J. D. Marth, M. Sperandio, Coordinated roles of ST3Gal-VI and ST3Gal-IV sialyltransferases in the synthesis of selectin ligands. *Blood* **120**, 1015–1026 (2012). doi: 10.1182/blood-2012-04-424366; pmid: 22700726
20. N. Kamada, S. U. Seo, G. Y. Chen, G. Nunez, Role of the gut microbiota in immunity and inflammatory disease. *Nat. Rev. Immunol.* **13**, 321–335 (2013). doi: 10.1038/nri3430; pmid: 23618829
21. N. A. Nagalingam, S. V. Lynch, Role of the microbiota in inflammatory bowel diseases. *Inflamm. Bowel Dis.* **18**, 968–984 (2012). doi: 10.1002/ibd.21866; pmid: 21936031
22. N. Figueroa-Bossi, S. Uzzau, D. Maloriol, L. Bossi, Variable assortment of prophages provides a transferable repertoire of pathogenic determinants in *Salmonella*. *Mol. Microbiol.* **39**, 260–271 (2001). doi: 10.1046/j.1365-2958.2001.02234.x; pmid: 11136448
23. E. Monti *et al.*, Sialidases in vertebrates: A family of enzymes tailored for several cell functions. *Adv. Carbohydr. Chem. Biochem.* **64**, 403–479 (2010). doi: 10.1016/S0065-2318(10)64007-3; pmid: 20837202
24. W. H. Yang *et al.*, An intrinsic mechanism of secreted protein aging and turnover. *Proc. Natl. Acad. Sci. U.S.A.* **112**, 13657–13662 (2015). doi: 10.1073/pnas.1515464112; pmid: 26489654
25. A. Poltorak *et al.*, Defective LPS signaling in C3H/HeJ and C57BL/10ScCr mice: Mutations in *Tlr4* gene. *Science* **282**, 2085–2088 (1998). doi: 10.1126/science.282.5396.2085; pmid: 9851930
26. B. Beutler, Endotoxin, toll-like receptor 4, and the afferent limb of innate immunity. *Curr. Opin. Microbiol.* **3**, 23–28 (2000). doi: 10.1016/S1369-5274(99)00046-6; pmid: 10679425
27. M. T. Abreu, Toll-like receptor signalling in the intestinal epithelium: How bacterial recognition shapes intestinal function. *Nat. Rev. Immunol.* **10**, 131–144 (2010). doi: 10.1038/nri2707; pmid: 20098461
28. H. Huhta *et al.*, The expression of Toll-like receptors in normal human and murine gastrointestinal organs and the effect of microbiome and cancer. *J. Histochem. Cytochem.* **64**, 470–482 (2016). doi: 10.1369/0022155416656154; pmid: 27370795
29. R. Dheer *et al.*, Intestinal epithelial Toll-like receptor 4 signaling affects epithelial function and colonic microbiota and promotes a risk for transmissible colitis. *Infect. Immun.* **84**, 798–810 (2016). doi: 10.1128/IAI.01374-15; pmid: 26755160
30. C. L. Leaphart *et al.*, A critical role for TLR4 in the pathogenesis of necrotizing enterocolitis by modulating intestinal injury and repair. *J. Immunol.* **179**, 4808–4820 (2007). doi: 10.4049/jimmunol.179.7.4808; pmid: 17878380
31. A. Moscona, Neuraminidase inhibitors for influenza. *N. Engl. J. Med.* **353**, 1363–1373 (2005). doi: 10.1056/NEJMra050740; pmid: 16192481
32. K. Hata *et al.*, Limited inhibitory effects of oseltamivir and zanamivir on human sialidases. *Antimicrob. Agents Chemother.* **52**, 3484–3491 (2008). doi: 10.1128/AAC.00344-08; pmid: 18694948
33. N. M. Stamatos *et al.*, LPS-induced cytokine production in human dendritic cells is regulated by sialidase activity. *J. Leukoc. Biol.* **88**, 1227–1239 (2010). doi: 10.1189/jlb.1209776; pmid: 20826611

Downloaded from http://science.sciencemag.org/ on December 21, 2017

34. Y.-L. Huang, C. Chassard, M. Hausmann, M. von Itzstein, T. Hennet, Sialic acid catabolism drives intestinal inflammation and microbial dysbiosis in mice. *Nat. Commun.* **6**, 8141 (2015). doi: 10.1038/ncomms9141; pmid: 26303108
35. S. Ramasamy *et al*., Intestinal alkaline phosphatase has beneficial effects in mouse models of chronic colitis. *Inflamm. Bowel Dis.* **17**, 532–542 (2011). doi: 10.1002/ibd.21377; pmid: 20645323
36. T. Dolowschiak *et al*., IFN-γ hinders recovery from mucosal inflammation during antibiotic therapy for *Salmonella* gut infection. *Cell Host Microbe* **20**, 238–249 (2016). doi: 10.1016/j.chom.2016.06.008; pmid: 27453483
37. S. L. Foster, R. Medzhitov, Gene-specific control of the TLR-induced inflammatory response. *Clin. Immunol.* **130**, 7–15 (2009). doi: 10.1016/j.clim.2008.08.015; pmid: 18964303
38. K. Kamdar *et al*., Genetic and metabolic signals during acute enteric bacterial infection alter the microbiota and drive progression to chronic inflammatory disease. *Cell Host Microbe* **19**, 21–31 (2016). doi: 10.1016/j.chom.2015.12.006; pmid: 26764594
39. S. Manco *et al*., Pneumococcal neuraminidases A and B both have essential roles during infection of the respiratory tract and sepsis. *Infect. Immun.* **74**, 4014–4020 (2006). doi: 10.1128/IAI.01237-05; pmid: 16790774
40. S. M. Schwerdtfeger, M. F. Melzig, Sialidases in biological systems. *Pharmazie* **65**, 551–561 (2010). pmid: 20824954
41. A. Varki, P. Gagneux, Multifarious roles of sialic acids in immunity. *Ann. N. Y. Acad. Sci.* **1253**, 16–36 (2012). doi: 10.1111/j.1749-6632.2012.06517.x; pmid: 22524423
42. K. Yamaguchi *et al*., Regulation of plasma-membrane-associated sialidase *NEU3* gene by Sp1/Sp3 transcription factors. *Biochem. J.* **430**, 107–117 (2010). doi: 10.1042/BJ20100350; pmid: 20518744
43. W. Ma *et al*., The p38 mitogen-activated kinase pathway regulates the human interleukin-10 promoter via the activation of Sp1 transcription factor in lipopolysaccharide-stimulated human macrophages. *J. Biol. Chem.* **276**, 13664–13674 (2001). doi: 10.1074/jbc.M011157200; pmid: 11278848
44. V. S. Carl, J. K. Gautam, L. D. Comeau, M. F. Smith Jr., Role of endogenous IL-10 in LPS-induced STAT3 activation and IL-1 receptor antagonist gene expression. *J. Leukoc. Biol.* **76**, 735–742 (2004). doi: 10.1189/jlb.1003526; pmid: 15218058
45. Y. Kakugawa *et al*., Up-regulation of plasma membrane-associated ganglioside sialidase (Neu3) in human colon cancer and its involvement in apoptosis suppression. *Proc. Natl. Acad. Sci. U.S.A.* **99**, 10718–10723 (2002). doi: 10.1073/pnas.152597199; pmid: 12149448
46. S. Kawamura *et al*., Plasma membrane-associated sialidase (NEU3) regulates progression of prostate cancer to androgen-independent growth through modulation of androgen receptor signaling. *Cell Death Differ.* **19**, 170–179 (2012). doi: 10.1038/cdd.2011.83; pmid: 21681193
47. K. Yamaguchi *et al*., Reduced susceptibility to colitis-associated colon carcinogenesis in mice lacking plasma membrane-associated sialidase. *PLOS ONE* **7**, e41132 (2012). doi: 10.1371/journal.pone.0041132; pmid: 22815940
48. T. Wada *et al*., Cloning, expression, and chromosomal mapping of a human ganglioside sialidase. *Biochem. Biophys. Res. Commun.* **261**, 21–27 (1999). doi: 1006/bbrc.1999.0973; pmid: 10405317
49. A. Mozzi *et al*., NEU3 activity enhances EGFR activation without affecting EGFR expression and acts on its sialylation levels. *Glycobiology* **25**, 855–868 (2015). doi: 10.1093/glycob/cwv026; pmid: 25922362
50. K. Ohtsubo *et al*., Dietary and genetic control of glucose transporter 2 glycosylation promotes insulin secretion in suppressing diabetes. *Cell* **123**, 1307–1321 (2005). doi: 10.1016/j.cell.2005.09.041; pmid: 16377570
51. B. Weinhold *et al*., Genetic ablation of polysialic acid causes severe neurodevelopmental defects rescued by deletion of the neural cell adhesion molecule. *J. Biol. Chem.* **280**, 42971–42977 (2005). doi: 10.1074/jbc.M511097200; pmid: 16267048
52. P. K. Grewal *et al*., ST6Gal-I restrains CD22-dependent antigen receptor endocytosis and Shp-1 recruitment in normal and pathogenic immune signaling. *Mol. Cell. Biol.* **26**, 4970–4981 (2006). doi: 10.1128/MCB.00308-06; pmid: 16782884
53. K. Ohtsubo, J. D. Marth, Glycosylation in cellular mechanisms of health and disease. *Cell* **126**, 855–867 (2006). doi: 10.1016/j.cell.2006.08.019; pmid: 16959566
54. P. R. Crocker, J. C. Paulson, A. Varki, Siglecs and their roles in the immune system. *Nat. Rev. Immunol.* **7**, 255–266 (2007). doi: 10.1038/nri2056; pmid: 17380156
55. F.-T. Liu, G. A. Rabinovich, Galectins: Regulators of acute and chronic inflammation. *Ann. N. Y. Acad. Sci.* **1183**, 158–182 (2010). doi: 10.1111/j.1749-6632.2009.05131.x; pmid: 20146714
56. A. Tuin *et al*., Role of alkaline phosphatase in colitis in man and rats. *Gut* **58**, 379–387 (2009). doi: 10.1136/gut.2007.128868; pmid: 18852260
57. M. Lukas *et al*., Exogenous alkaline phosphatase for the treatment of patients with moderate to severe ulcerative colitis. *Inflamm. Bowel Dis.* **16**, 1180–1186 (2010). doi: 10.1002/ibd.21161; pmid: 19885903
58. K. Molnár *et al*., Intestinal alkaline phosphatase in the colonic mucosa of children with inflammatory bowel disease. *World J. Gastroenterol.* **18**, 3254–3259 (2012). doi: 10.3748/wjg.v18.i25.3254; pmid: 22783049
59. S. N. Alam *et al*., Intestinal alkaline phosphatase prevents antibiotic-induced susceptibility to enteric pathogens. *Ann. Surg.* **259**, 715–722 (2014). doi: 10.1097/SLA.0b013e31828fae14; pmid: 23598380
60. J. J. Miklavcic *et al*., Increased catabolism and decreased unsaturation of ganglioside in patients with inflammatory bowel disease. *World J. Gastroenterol.* **21**, 10080–10090 (2015). doi: 10.3748/wjg.v21.i35.10080; pmid: 26401073
61. R. F. Goldberg *et al*., Intestinal alkaline phosphatase is a gut mucosal defense factor maintained by enteral nutrition. *Proc. Natl. Acad. Sci. U.S.A.*. **105**, 3551–3556 (2008). doi: 10.1073/pnas.0712140105; pmid: 18292227
62. D. M. Heithoff *et al*., Intraspecies variation in the emergence of hyperinfectious bacterial strains in nature. *PLOS Pathog.* **8**, e1002647 (2012). doi: 10.1371/journal.ppat.1002647; pmid: 22511871
63. J. Fu *et al*., Loss of intestinal core 1-derived *O*-glycans causes spontaneous colitis in mice. *J. Clin. Invest.* **121**, 1657–1666 (2011). doi: 10.1172/JCI45538; pmid: 21383503
64. S. Narisawa *et al*., Accelerated fat absorption in intestinal alkaline phosphatase knockout mice. *Mol. Cell. Biol.* **23**, 7525–7530 (2003). doi: 10.1128/MCB.23.21.7525-7530.2003; pmid: 14560000
65. K. Ohtsubo, M. Z. Chen, J. M. Olefsky, J. D. Marth, Pathway to diabetes through attenuation of pancreatic beta cell glycosylation and glucose transport. *Nat. Med.* **17**, 1067–1075 (2011). doi: 10.1038/nm.2414; pmid: 21841783
66. L. G. Ellies *et al*., Sialyltransferase ST3Gal-IV operates as a dominant modifier of hemostasis by concealing asialoglycoprotein receptor ligands. *Proc. Natl. Acad. Sci. U.S.A.* **99**, 10042–10047 (2002). doi: 10.1073/pnas.142005099; pmid: 12097641
67. M. R. Davis Jr., J. B. Goldberg, Purification and visualization of lipopolysaccharide from Gram-negative bacteria by hot aqueous-phenol extraction. *J. Vis. Exp.* **2012**, 3916 (2012). doi: 10.3791/3916; pmid: 22688346
68. C.-H. Lee, C.-M. Tsai, Quantification of bacterial lipopolysaccharides by the purpald assay: Measuring formaldehyde generated from 2-keto-3-deoxyoctonate and heptose at the inner core by periodate oxidation. *Anal. Biochem.* **267**, 161–168 (1999). doi: 10.1006/abio.1998.2961; pmid: 9918668
69. N. J. Foot *et al*., *Ndfip1*–deficient mice have impaired DMT1 regulation and iron homeostasis. *Blood* **117**, 638–646 (2011). doi: 10.1182/blood-2010-07-295287; pmid: 20959604.
70. A. Fuhrer *et al*., Milk sialyllactose influences colitis in mice through selective intestinal bacterial colonization. *J. Exp. Med.* **207**, 2843–2854 (2010). doi: 10.1084/jem.20101098; pmid: 21098096
71. M. H. Zaki *et al*., The NLRP3 inflammasome protects against loss of epithelial integrity and mortality during experimental colitis. *Immunity* **32**, 379–391 (2010). doi: 10.1016/j.immuni.2010.03.003; pmid: 20303296

ACKNOWLEDGMENTS

This research was funded by NIH grants HL125352 (J.D.M. and V.N.) and HL131474 (J.D.M., M.J.M., and V.N.). Additional support was provided by the Wille Family Foundation (J.D.M.) and by SFB914 from the German Research Foundation (M.S.). The data presented in this study are in the main text and in the Supplementary Materials. W.H.Y., D.M.H., P.V.A., M.J.M., and J.D.M. designed the experimental strategies. J.D.M. and M.J.M. supervised the project. W.H.Y., D.M.H., and P.V.A. performed the experiments and acquired data. All authors contributed to data analysis and manuscript preparation. The authors declare that they have no competing interests.

SUPPLEMENTARY MATERIALS

www.sciencemag.org/content/358/6370/eaao5610/suppl/DC1
Figs. S1 to S10

4 August 2017; accepted 13 November 2017
10.1126/science.aao5610

Downloaded from http://science.sciencemag.org/ on December 21, 2017

Science

Recurrent infection progressively disables host protection against intestinal inflammation

Won Ho Yang, Douglas M. Heithoff, Peter V. Aziz, Markus Sperandio, Victor Nizet, Michael J. Mahan and Jamey D. Marth

Science **358** (6370), eaao5610.
DOI: 10.1126/science.aao5610

Minor infections cause big problems

Pathogenic infection has been implicated in the chronic inflammation seen in inflammatory bowel diseases (IBDs) such as ulcerative colitis and Crohn's disease. Yang *et al.* show that recurrent, low-level, and fully resolving *Salmonella enterica* Typhimurium (ST) infections can precipitate severe colonic inflammation in mice. ST-induced TLR4 activation resulted in increased neuraminidase 3 (Neu3) production and activity in the duodenum. This led to intestinal alkaline phosphatase (IAP) desialylation and degradation. IAP deficiency caused a marked increase in commensal bacteria-generated lipopolysaccharide-phosphate in the colon, provoking inflammation. Treatment with calf IAP or the antiviral drug zanamivir (which inhibits Neu3 activity) prevented this inflammatory cascade. This pathway may serve as an effective target for future human IBD therapies.

Science, this issue p. eaao5610

ARTICLE TOOLS http://science.sciencemag.org/content/358/6370/eaao5610

SUPPLEMENTARY MATERIALS http://science.sciencemag.org/content/suppl/2017/12/20/358.6370.eaao5610.DC1

RELATED CONTENT
http://stm.sciencemag.org/content/scitransmed/9/416/eaah6888.full
http://stm.sciencemag.org/content/scitransmed/9/380/eaaf9044.full
http://stm.sciencemag.org/content/scitransmed/6/225/225ra28.full
http://stm.sciencemag.org/content/scitransmed/4/158/158ra144.full

REFERENCES This article cites 71 articles, 22 of which you can access for free
http://science.sciencemag.org/content/358/6370/eaao5610#BIBL

PERMISSIONS http://www.sciencemag.org/help/reprints-and-permissions

Use of this article is subject to the Terms of Service

Science (print ISSN 0036-8075; online ISSN 1095-9203) is published by the American Association for the Advancement of Science, 1200 New York Avenue NW, Washington, DC 20005. 2017 © The Authors, some rights reserved; exclusive licensee American Association for the Advancement of Science. No claim to original U.S. Government Works. The title *Science* is a registered trademark of AAAS.

Downloaded from http://science.sciencemag.org/ on December 21, 2017